Quaternary Science Reviews 29 (2010) 832–846

Contents lists available at ScienceDirect

Quaternary Science Reviews

journal homepage: www.elsevier.com/locate/quascirev

Late Matuyama climate forcing on sedimentation at the margin of the southern Alps (Italy)

Giancarlo Scardia [a,*], Marta Donegana [b], Giovanni Muttoni [c,d], Cesare Ravazzi [b], Giovanni Vezzoli [e]

[a] Istituto Nazionale di Geofisica e Vulcanologia, Sezione di Milano-Pavia, Via Bassini 15, I-20133 Milano, Italy
[b] CNR-IDPA, Piazza della Scienza 1, I-20126 Milano, Italy
[c] Dipartimento di Scienze della Terra, Università degli Studi di Milano, Via Mangiagalli 34, I-20133 Milano, Italy
[d] ALP – Alpine Laboratory of Paleomagnetism, Via Madonna dei Boschi 76, I-12016 Peveragno (CN), Italy
[e] Dipartimento di Scienze Geologiche e Geotecnologie, Università di Milano-Bicocca, Piazza della Scienza 4, I-20126 Milano, Italy

ARTICLE INFO

Article history:
Received 7 September 2009
Received in revised form
30 November 2009
Accepted 1 December 2009

ABSTRACT

The Pleistocene history of climate control on sedimentation in the Southern Alps–Po Plain system, northern Italy, was reconstructed using an integrated magnetostratigraphic, palynological, and petrographical approach on a 47-m-deep core. The core mainly consists of lacustrine sediments pertaining to the Bagaggera sequence, deposited at the foothills of the Southern Alps during the late Matuyama subchron (0.99–0.78 Ma). At that time, climate worsened globally and locally it caused the progradation of an alluvial fan unit onto the nearby Po Plain, triggering lake formation by damming of a tributary valley. These new data are used in conjunction with data from the literature to highlight and track the effects of climate forcing on sedimentation during the late Matuyama subchron in different orographic and geodynamic settings of the Southern Alps–Po Plain system as part of the greater Alpine area. We found that the episodes of alluvial fan and braidplain progradation observed in the southern foreland of the Alps during the late Matuyama global cooling seem broadly synchronous with the deposition of most of the so-called Günz and Älterer Deckenschotter deposits in the northern forelands of the Alps as well as with the first major waxing of the Alpine valley glaciers, possibly around the Marine Isotope Stage 22 (~0.87 Ma).

1. Introduction

Glacial stages in mountain environments are characterized by waxing of valley glaciers, enhanced erosion, and an overall reduction of vegetation cover, triggered by increased aridity and drop of temperatures. Enhanced erosion typically results in intense production of sediments, arranged in morainic complexes or alluvial fans at the foothills of the glaciated mountain range, whilst, more distally, braided river systems prograde onto foreland plains.

Morainic complexes are by far the most studied markers of glacial advances, but their emplacement normally results in the obliteration of older complexes deposited by less extensive glacial advances (Gibbons et al., 1984). It is presumably for this reason that the Pleistocene record of Alpine glaciations, as revealed by the distribution of morainic complexes, seems incomplete compared to the number of sea-level lowstands inferred from the marine $\delta^{18}O$ record (Head and Gibbard, 2005).

Less attention has been generally paid on the progradation of alluvial fans as indicator of enhanced glacial activity, essentially because alluvial fans can originate from processes other than climatic (e.g., tectonic), with no compelling criteria for choosing among them provided by the sole study of their constituent lithofacies or petrofacies. Solving the ambiguities about the origin of alluvial fans requires the ability to date them in expanded and continuous sedimentary sequences and to characterize their palaeoenvironmental boundary conditions. To this end, the integrated approach of magnetostratigraphy, pollen analysis, and sediment petrography has been recently applied to date the onset of an episode of generalized braidplain progradation taking place in northern Italy during the late Matuyama subchron (0.99–0.78 Ma; time scale of Berggren et al., 1995 is used throughout), and to correlate this event to the glacio-eustatic lowstand of Marine Isotope Stage (MIS) 22 at ~0.87 Ma, which marked the first major Pleistocene glacial advance in the Alps (Muttoni et al., 2003, 2007). As a further case study, we present in this paper the results of a multidisciplinary study on a Pleistocene continental core comprised mainly of lacustrine deposits from the southern foothills of the Alps in northern Italy. Based on magnetostratigraphic, palynological, petrographical, and facies analyses, we depict the geological and

* Corresponding author. Tel.: +39 02 23699 455; fax: +39 02 23699 458.
E-mail address: scardia@mi.ingv.it (G. Scardia).

0277-3791/$ – see front matter © 2009 Elsevier Ltd. All rights reserved.
doi:10.1016/j.quascirev.2009.12.002

climatic evolution of the southern margin of the Alps during the late Matuyama subchron, when climate cooled globally and locally caused the progradation of an alluvial fan unit onto the nearby Po Plain, triggering lake formation by damming of a tributary valley. These new data are used in conjunction with data from the literature to augment our knowledge on the regional geological, paleobiological, and climatical evolution of the Po Plain and the greater Alpine area during the early stages of the major Pleistocene glaciations in the Alps (e.g., Muttoni et al., 2003).

2. Study area and geological background

The study area is located ~30 km northeast of Milan (Fig. 1). The bedrock mainly consists of two lithostratigraphic units, the Bergamo Flysch (Campanian; Galbiati, 1969; Bersezio and Fornaciari, 1994) and the Scaglia Lombarda Group (Maastrichtian–Lutetian; Kleboth, 1982), arranged in south-verging syncline-anticline structures. The bedrock, folded and eroded, is overlain by a complex association of Pliocene–Pleistocene deposits (Fig. 1). The oldest outcropping unit consists of Early–Middle Pliocene marine to continental fine-grained sediments (Pini et al., 2003), exposed a few kilometres southeast of the study area along the Adda River bed, overlain by a ~100-m-thick succession of poorly dated Late Pliocene?–Middle Pleistocene fluvial conglomerates exposed along the terrace scarps of the Adda, Molgora, and Curone rivers (Orombelli, 1979) (Fig. 1). Petrographical studies on gravels allowed to recognize different sources of provenance of these conglomerates, pointing to a complex regional evolution of their catchment areas during the Late Pliocene?–Middle Pleistocene (Orombelli and Gnaccolini, 1978). Since the onset of the major Pleistocene glaciations (~0.87 Ma; Muttoni et al., 2003), the whole area experienced repeated advances of the Adda glacier *s.l.*, as testified by the widespread occurrence of Middle–Late Pleistocene glacial deposits (Venzo, 1948; Riva, 1957; Cremaschi, 1987; Strini, 2001; Bini et al., 2004), save for the Curone Valley (Fig. 1), where a quite different succession is preserved.

The Curone Valley was never occupied by Pleistocene glaciers and hosted mainly lacustrine, fluvial, and loess deposits pertaining to the so-called Bagaggera sequence, first described by Venzo (1948, 1952). The Bagaggera sequence was analyzed for paleomagnetism between the late '70s and the early '80s in the framework of the IGCP project 73/1/24. A magnetic polarity reversal was recognized in the lacustrine deposits and referred to the Brunhes–Matuyama boundary (0.78 Ma) (Bucha and Šibrava, 1977; Billard et al., 1983) or to the middle Matuyama–Jaramillo boundary (1.07 Ma) (Cremaschi et al., 1985). Cremaschi et al. (1985) also applied paleopedological and petrographical analyses to recognize in the Bagaggera sequence the presence of five Middle–Late Pleistocene glacial phases. At the top of the Bagaggera sequence, a burnt flint recovered from the uppermost loess layers was dated to 60.5 ± 7.5 ka by means of thermoluminescence (Cremaschi et al., 1990). Orombelli (1979) firstly suggested that the lacustrine deposits of the Bagaggera sequence were originated by the fluvial damming of the Curone Valley, but the causes

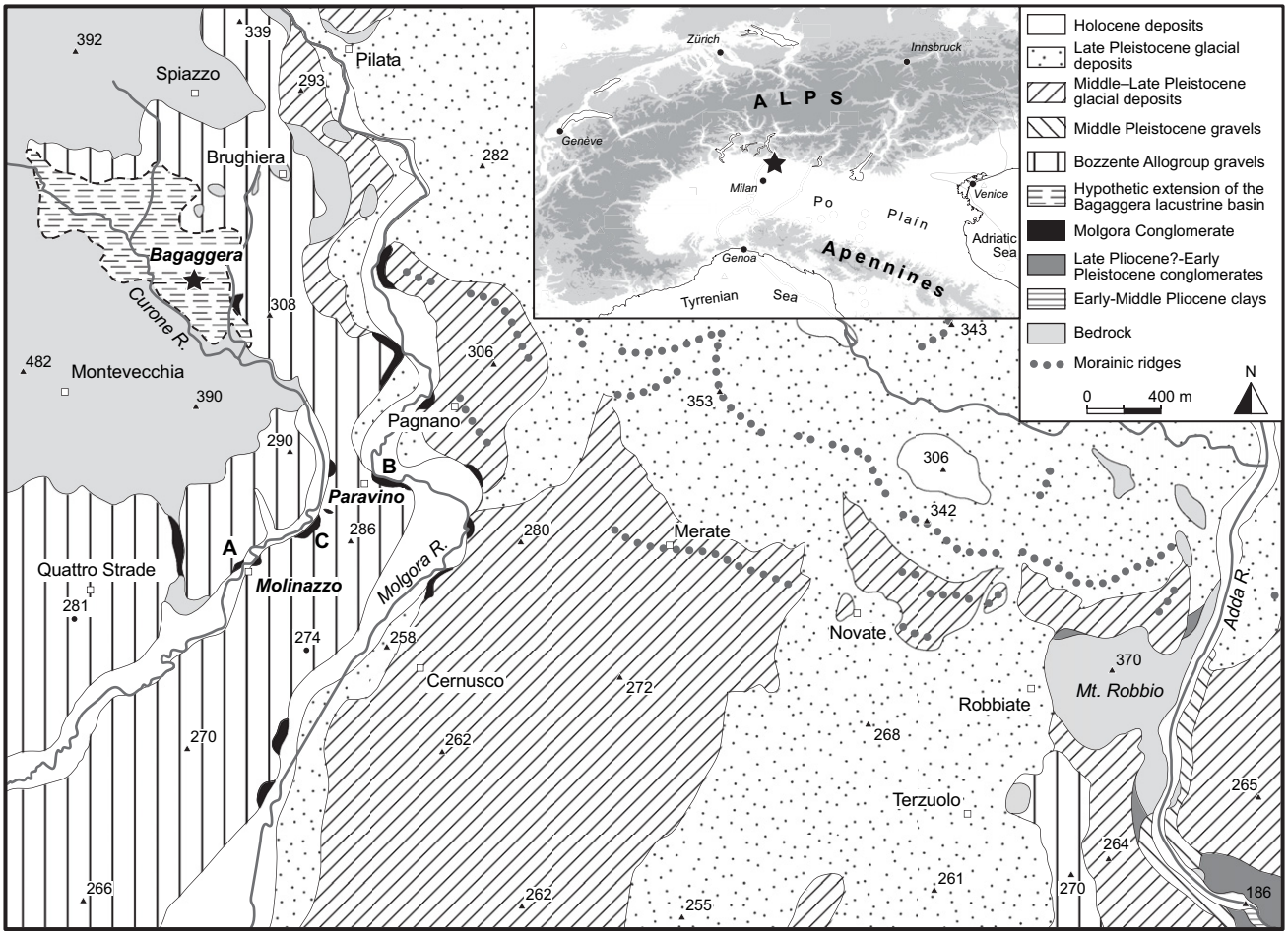

Fig. 1. Simplified geologic map of the study area from Venzo (1948), Strini (2001), and this study. The Bagaggera RL17 drill site and the outcrops of the Paravino composite section are shown with a star and letters (A, B, C), respectively. The presumed extension of lake Bagaggera is also displayed.

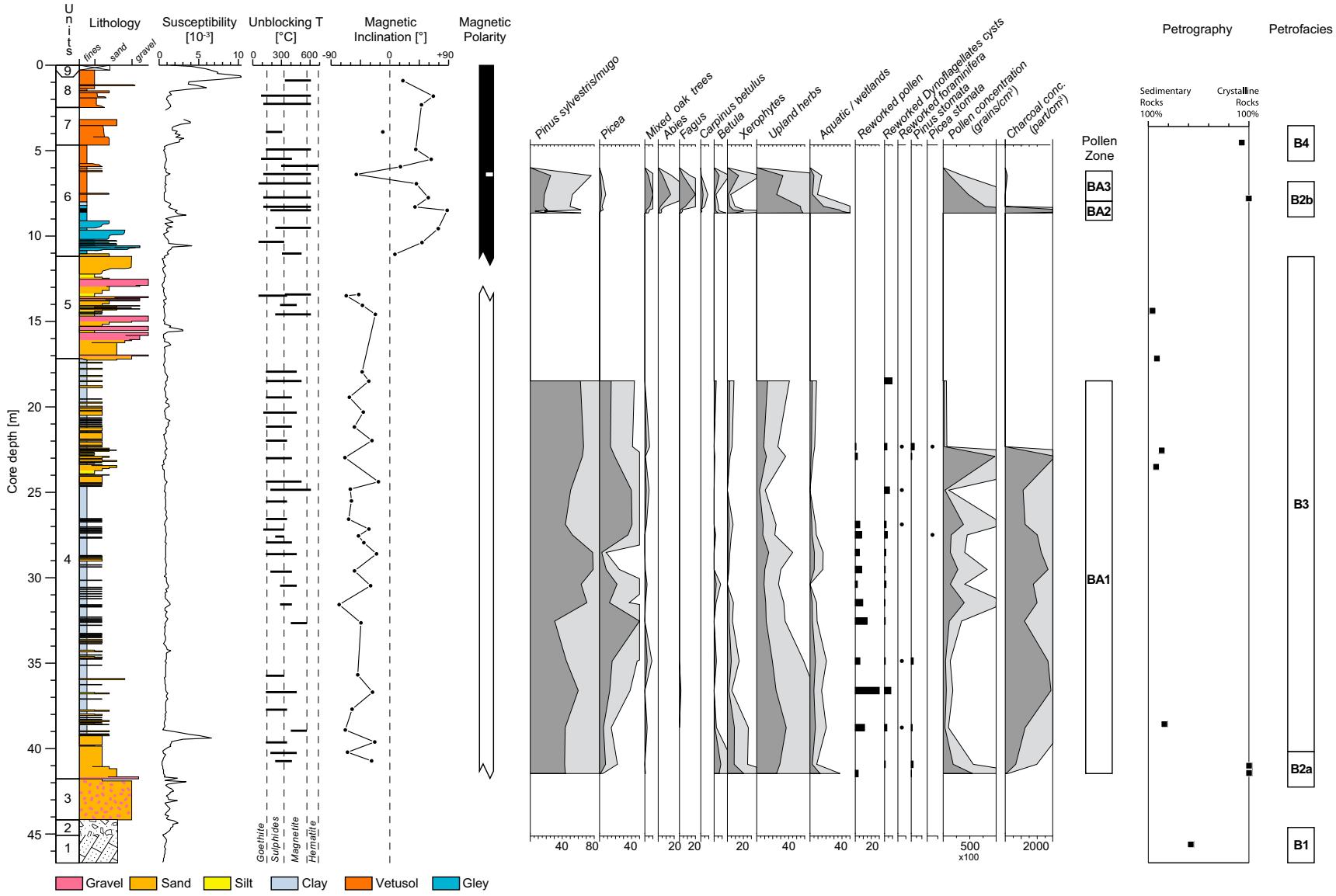

Fig. 2. From left to the right: stratigraphic units, lithology, low field susceptibility curve, unblocking temperatures of the characteristic remanent magnetization component, magnetic inclination values, magnetostratigraphy, pollen diagram, and petrography of the core RL17. The magnetostratigraphy was retrieved from the inclination of the characteristic component vectors expressed in degrees from horizontal; black is normal polarity, white is reverse polarity.

(e.g., climatic *versus* tectonic) and age of damming and lacustrine deposition could not be unambiguously determined.

3. Lithostratigraphy of the Bagaggera basin

The Bagaggera sequence was well exposed along quarry walls until the exploitation activity for brick production ended in the late '80s. Cremaschi et al. (1985) benefited at that time from the presence of extended exposures and were able to recognize the existence of two sub-basins. A shallower sub-basin located toward the northern bank of the Curone Valley and mainly characterized by a ~15-m-thick succession of slope deposits, fluvial gravels, and loess, and a deeper sub-basin located more southward roughly along the axial sector of the Curone Valley and hosting a thicker sedimentary sequence with lacustrine to fluvial deposits. We investigated the southern, thicker sub-basin by recovering the whole sedimentary succession present therein with a 47-m-long core, hereafter referred to as core RL17 (Figs. 1, 2; Table 1). A detailed facies description of core RL17 is provided in Appendix A; in summary, core RL17 mainly consists, from bottom to top, of a chaotic package of monogenic coarse-grained sand and pebbles (Unit 3) followed by a ~25-m-thick succession of silty clay with sand layers of lacustrine origin (Unit 4), overlain with erosional contact by gravels with petrographical composition indicating local provenance and attributed to an alluvial fan (Unit 5). Above there are sands and silty clay attributed to swamp/lacustrine settings (Unit 6), and sands attributed to fluvial settings (Unit 7), sealed by a polycyclic, reworked loess cover (Unit 8). The base of Unit 6 displays strong blue to green hues, suggesting hydromorphy and oxygen depletion. The uppermost section of the core (Units 6–8) is strongly affected by prolonged and polycyclic weathering responsible for the formation of a vetusol (Cremaschi, 1987), characterized by decalcification and oxidation fronts located at ~7 m and ~8 m from the ground surface, respectively.

At the Curone Valley outlet, along the Curone and Molgora river scarps, a succession of superimposed coarse-grained deposits crops out (Venzo, 1948; Orombelli, 1979; Strini, 2001; Bini et al., 2004). This succession, studied in the Paravino composite section (comprised of three overlapping subsections; Fig. 1; Table 1; detailed facies description in Appendix A), starts at the bottom (Molinazzo subsection; Fig. 3) with fine-grained sediments of proximal overbank or abandoned channel facies (Molgora Conglomerate) passing upward (Molgora River sub-section; Fig. 3) to a stack of coarse-grained conglomerates (Molgora Conglomerate). Above (Paravino subsection; Fig. 3) lie, with a very irregular and undulated contact (the so-called *geologische Orgeln*; Penck and Brückner, 1909; Orombelli, 1979; Bini et al., 2004), coarse-grained, massive, and strongly weathered gravels (Bozzente Allogroup), sealed by loess deposits.

Table 1
Core Bagaggera RL17 and outcrops data.

Name	Drill/Outcrop site [a]	Depth [b]	Core recovery	Samples collected[c]		
				Pm	Pl	Pg
Bagaggera RL17	45°42'38.1″ 9°23'04.7″	47	95%	49	37	10
Paravino[d]	45°41'53.1″ 9°23'32.0″	–	–	–	–	3
Molgora River[d]	45°42'03.2″ 9°23'50.8″	–	–	–	–	4
Molinazzo[d]	45°41'50.7″ 9°23'17.1″	–	–	7	2	1

[a] Drill/outcrop site - latitude and longitude in degrees according to the WGS84 reference system.
[b] Total depth of core from the site surface, in meters.
[c] Number of samples collected for paleomagnetic (Pm), palinologic (Pl), and petrographic (Pg) analyses, respectively.
[d] sub-sections of the Paravino composite section.

4. Palynology

4.1. The Bagaggera sequence (core RL17)

Samples for palynology were treated according to standard methods (including HF and acetolysis). *Lycopodium* tablets (Stockmarr, 1971) were added to estimate pollen and charcoal concentration. Identification of pollen types was made with reference to Moore et al. (1991), Punt and Blackmore (1976–2004), Reille (1992–1995), Beug (2004), and the reference collection of the Laboratory of Palynology and Palaeoecology of CNR-IDPA (Istituto per la Dinamica dei Processi Ambientali; Milan, Italy). Nomenclature of pollen types follows ALPADABA (Alpine Palynological Database; Bern, Switzerland); microfossils were named after van Geel (1978) and van Geel et al. (1981), whereas fossil conifer stomata after Trautmann (1953). Pollen percentages are based on a pollen sum of 300 grains pertaining to trees, shrubs, and upland herbs; pollen of aquatic and mire species, algae, microfossils, spores of Pteridophytes, and reworked pollen grains (see below) have been excluded from the pollen sum used for calculation of percentage values.

A total of 37 samples from core RL17 have been analyzed (Table 1). Lacustrine Unit 4 is characterized by an overall low pollen concentration (10^2–10^3 grains/cm^3) and well-preserved primary pollen grains, whereas the preservation degree in the somewhat richer (10^4 grains/cm^3) swamp/lacustrine Unit 6 is variable. Oxidized and hydromorphic sediments in the 14.5–10.4 m interval (Unit 5 and base of Unit 6) were found barren of pollen. A total of 3 pollen zones have been recognized from base to top using percentage pollen abundances (Fig. 2).

4.1.1. Zone BA1

This zone is dominated by conifer trees (*Pinus sylvestris/mugo* plus *Picea* > 50%) and herb pollen (Gramineae and Compositae) including steppe plants (*Hippophäe, Ephedra fragilis* type, Chenopodiaceae, *Helianthemum*). *Alnus* and *Betula* are scarce, while the occurrence of Cyperaceae pollen can be related to local perilacustrine vegetation. Pollen of *Larix* is also present, though sporadically. This pollen association is attributed to steppe–taiga ecotones of cold–temperate continental climates, which are typical of the Southern Alps margin during Pleistocene cold stages (Ravazzi and Rossignol Strick, 1995; Ravazzi et al., 2005; Monegato et al., 2007). This type of vegetation persisted over the entire time span corresponding to the deposition of the lacustrine succession (Unit 4). Reworked pollen grains of *Symplocos*, Taxodiaceae, and Juglandaceae occur regularly throughout zone BA1. These taxa were common in the Pliocene–Early Pleistocene of the Southern Alps margin (Pini et al., 2003), and their occurrence in the Bagaggera basin suggests erosion of former Pliocene–Early Pleistocene deposits.

4.1.2. Zone BA2

This zone is dominated by terrestrial herbs and xerophytes (>50%) with subordinate conifers and broad-leaved trees never exceeding 25%. Aquatic and wetland vegetation (Cyperaceae, *Myriophyllum*, and *Ranunculus acris* type) is very abundant. This pollen assemblage deposited in a swamp hosting aquatic and terrestrial vegetation, surrounded by an open, mixed forest of warm-temperate climate.

4.1.3. Zone BA3

In this zone, the arboreal pollen increases, but herbs are still abundant. *Pinus, Abies,* and *Fagus* are associated with thermophilous broad-leaved trees such as *Corylus*, *Quercus*, *Carpinus betulus*, *Tilia*, and *Ulmus*. A denser, mixed forest of warm and moist temperate climate surrounded a swamp during the time span represented by

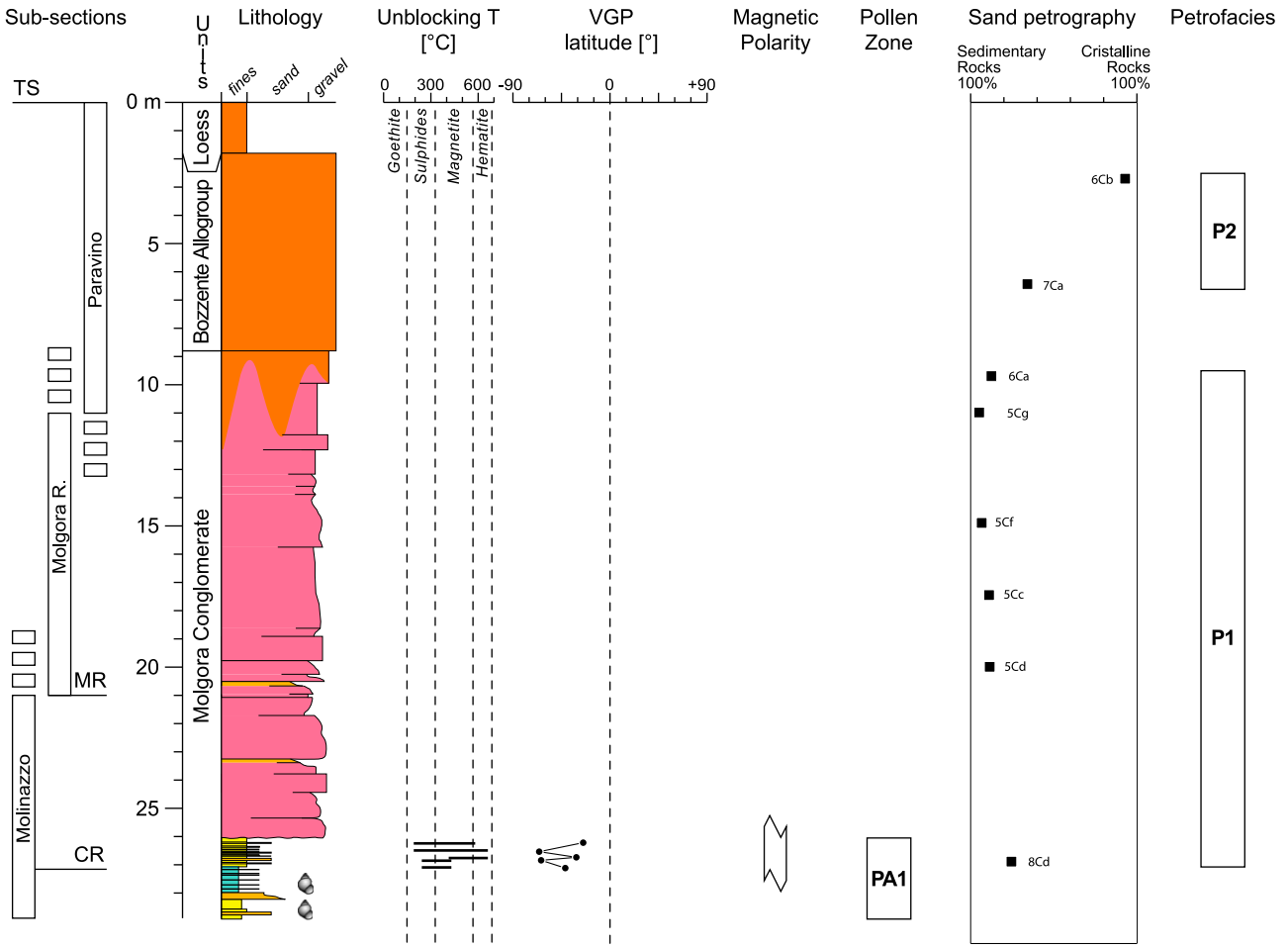

Fig. 3. From left to the right: sub-sections, stratigraphic units, lithology, unblocking temperatures of the characteristic remanent magnetization component, virtual geomagnetic pole (VGP) latitudes, magnetostratigraphy, palinology, and petrography of the Paravino composite section. Negative VGP latitudes indicate reverse polarity. TS: Paravino terrace surface; MR: Molgora River; CR: Curone River.

zone BA3. This pollen assemblage fits the composition of the coalified plant remains included in the so-called "Mindel-Riss clay" mentioned by Venzo (1948, p. 92) from a nearby outcrop section.

4.2. The paravino composite section

The fine-grained alluvial sediments interbedded in the Molgora Conglomerate and exposed at the base of the Paravino composite section (Fig. 3) provided a low concentration (15–20 grains/cm^3) pollen assemblage characterized by *Pinus sylvestris/mugo, Picea, Juniperus,* Gramineae, and pollen of *Symplocos* presumably reworked from Pliocene–Early Pleistocene deposits. This assemblage is similar to the assemblage of basal zone BA1 in the Bagaggera sequence, and suggests that the sedimentation of the Molgora Conglomerate occurred under cold to cold-temperate climate conditions.

4.3. Climatostratigraphic overview of the pollen record

The ~25-m-thick detrital lacustrine succession of the Bagaggera sequence (Unit 4) contains a uniform pollen assemblage typical of steppe-taiga environments, suggesting that a cold-continental climate persisted during the entire time span of lacustrine deposition. Similar conclusions can be drawn for the pollen content of the fine-grained deposits comprised within the Molgora Conglomerate at the base of the Paravino composite section. We therefore argue that lake Bagaggera was formed during a single phase of cold climate. Steppe-taiga vegetation with conifers including *Larix* characterized Pleistocene glacial stages at the southern margin of the Alps (Ravazzi and Rossignol Strick, 1995; Ravazzi et al., 2005; Monegato et al., 2007; Muttoni et al., 2007; Pini et al., 2009). The sedimentary record at Bagaggera is consistent with a prolonged phase of extreme cold climate, which can be related to the full development of an even-numbered Marine Isotope Stage rather than a short-lived, higher frequency cooling episode of Pleistocene climate variability (Jouzel et al., 2007; Tzedakis, 2007).

Pollen zones BA2 and BA3 (Unit 6) indicate the presence of broad-leaved forests of *Corylus*, *Quercus*, *Carpinus betulus*, *Tilia*, *Ulmus,* and *Abies* thriving in warm-temperate climate. These forest types, lacking taxa typical of the Early Pleistocene (e.g. *Tsuga, Cedrus, Juglans* sect. *Cardiocaryon*; Ravazzi and Rossignol Strick, 1995; Müllenders et al., 1996; Kent et al., 2002; Muttoni et al., 2007), are recognized in several Middle–Late Pleistocene interglacial phases from the circum-Alpine region. Based on the absence in pollen zones BA2 and BA3 of *Carya* and *Pterocarya*, which have been found in northern Italy interglacial deposits as young as early Middle Pleistocene in age (Müllenders et al., 1996; Kent et al., 2002; Rossi, 2003), coupled with the abundance of *Fagus*, which is absent in northern Italy during the Eemian (MIS 5e) (Pini et al., 2009), we attribute pollen zones BA2 and BA3 to a Middle Pleistocene interglacial stage broadly comprised between MIS 15 and MIS 7 (~0.6–0.18 Ma).

5. Paleomagnetism

Paleomagnetic properties were studied on 49 cubic (~8 cm^3) and 7 cylindrical (~10 cm^3) samples collected from core RL17 and the Paravino section, respectively (Figs. 2 and 3; Table 1). About one sample every core-meter was taken in core RL17, whereas in the Paravino section only the bottom part of the section, bearing fine-grained sediments, could be sampled. The initial magnetic susceptibility of core RL17 was measured with a Bartington MS2 susceptibility bridge mounting a MS2C sensor. Paleomagnetic analyses were carried out at the Alpine Laboratory of Paleomagnetism (Peveragno, Italy). Samples were thermally demagnetized with an ASC TD48 oven. The natural remanent magnetization (NRM) was measured on a 2G-Enterprises DC-SQUID cryogenic magnetometer located in a magnetically shielded room with ambient fields of ~300 nT.

The susceptibility log of core RL17 (Fig. 2) shows that the detrital lacustrine sequence of Unit 4 (41.90–17.30 m) has rather homogeneous susceptibility values of around 2 10^{-3} SI, embedding a basal peak of up to 7 10^{-3} SI (39.5–39.2 m) possibly due to organic matter accumulation and sulphides formation (see also Appendix A). The rather homogeneous susceptibility values of Unit 4 point to deposition under a relatively constant sediment accumulation rate. The highest susceptibility values (4–10 10^{-3} SI) occur in the vetusol at the core top (4.7–0.3 m; Units 7 and 8; Fig. 2), probably enriched in magnetic minerals of pedogenic origin.

Magnetic mineralogy analyses were performed on representative samples from core RL17 and the Paravino composite section by means of isothermal remanent magnetization (IRM) acquisition curves and thermal decay of a three component IRM imparted at 0.12, 0.4, and 2.5 T fields (Lowrie, 1990) with an ASC pulse magnetizer. Two types of IRM acquisition curves were observed (Fig. 4): (i) IRM increased steeply and reached saturation at ~0.5 T fields (e.g., sample RL17-42.4, Unit 3); this behaviour is interpreted as resulting from the occurrence of a low coercivity phase such as magnetite. (ii) IRM continued to climb gently with no tendency to saturate even in a field of 2.5 T (e.g., samples RL17-12.45 and RL17-14.6, Unit 5); this behaviour is interpreted as resulting from the occurrence of high coercivity phases such as hematite and/or goethite. The thermal decay of a three component IRM shows that the most weathered intervals (i.e. the vetusol at the core top and the alluvial fan sediments of Unit 5) bear high coercivity component with maximum unblocking temperatures of ~680 °C interpreted as hematite; this mineral is found in association with a low coercivity component with maximum unblocking temperatures around ~570 °C, interpreted as magnetite (Fig. 5, sample RL17-2.4, vetusol; sample RL17-14.6, Unit 5). Samples from lacustrine Unit 4 are characterized by a drop of IRM intensity observed in the low, medium, and high coercivity curves between 350 and 400 °C, followed by a low IRM intensity tail up to 570 °C (Fig. 5, sample RL17-27.51, Unit 4). These properties are interpreted as due to the presence of dominant greigite (Fe_3S_4) that has been shown to possess maximum unblocking temperatures up to 350–360 °C (Sagnotti and Winkler, 1999), in association with subsidiary amounts of magnetite with maximum unblocking temperature of 570 °C. In the Paravino composite section, the magnetic mineralogy consists of a high coercivity component with maximum unblocking temperature of ~680 °C, interpreted as hematite (Fig. 5, samples MOL5 and MOL7).

The intensity of the NRM in samples from core RL17 and the Paravino section is in the 10^{-4}–10^{-3} A/m range with only a few samples from core RL17 in the 10^{-2} A/m range. Thermal demagnetization was carried out on all samples adopting a minimum of 15 steps from 80 to 600 °C, occasionally up to 680 °C. Standard least-square analysis (Kirschvink, 1980) was used to calculate component directions from selected linear segments of orthogonal projections of thermal demagnetization data (Zijderveld, 1967). In core RL17,

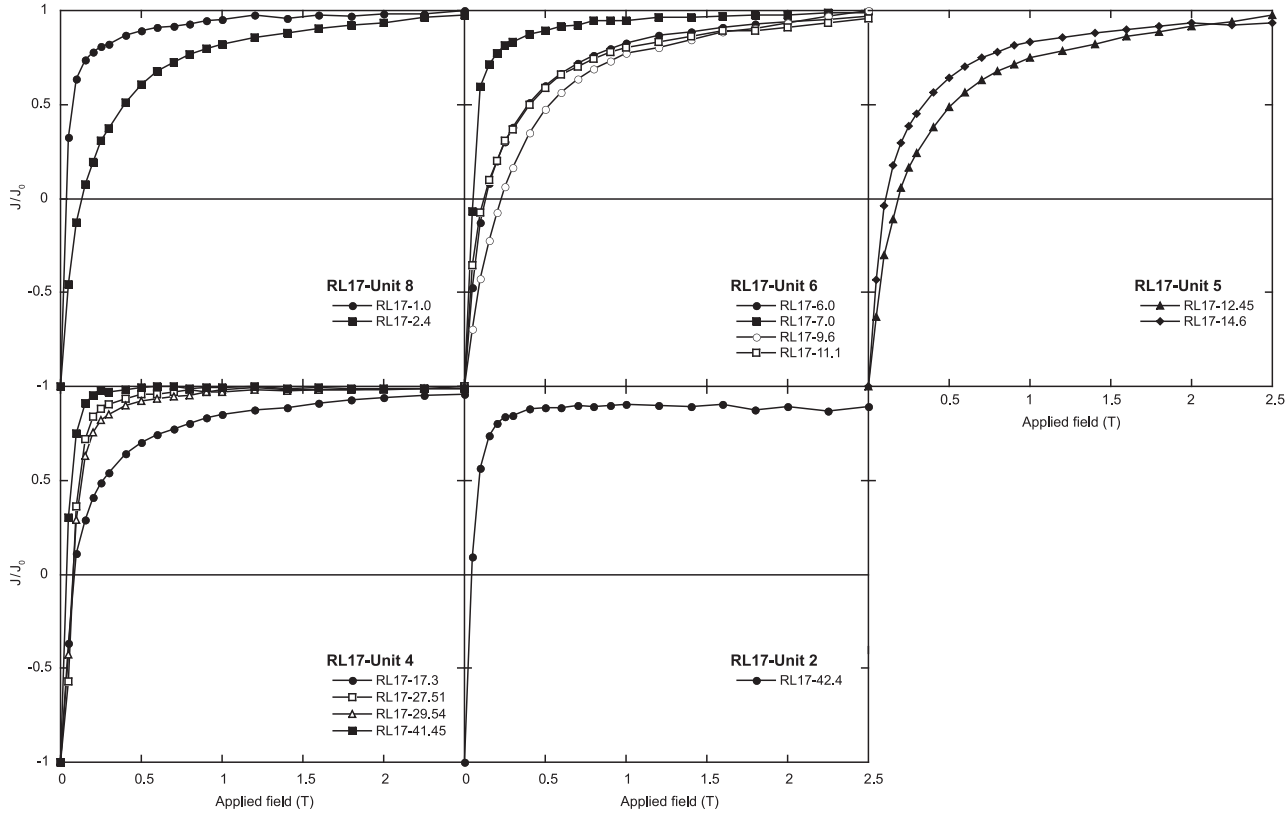

Fig. 4. Isothermal remanent magnetization (IRM) acquisition curves on representative samples from core RL17 and the Paravino composite section. See text for discussion.

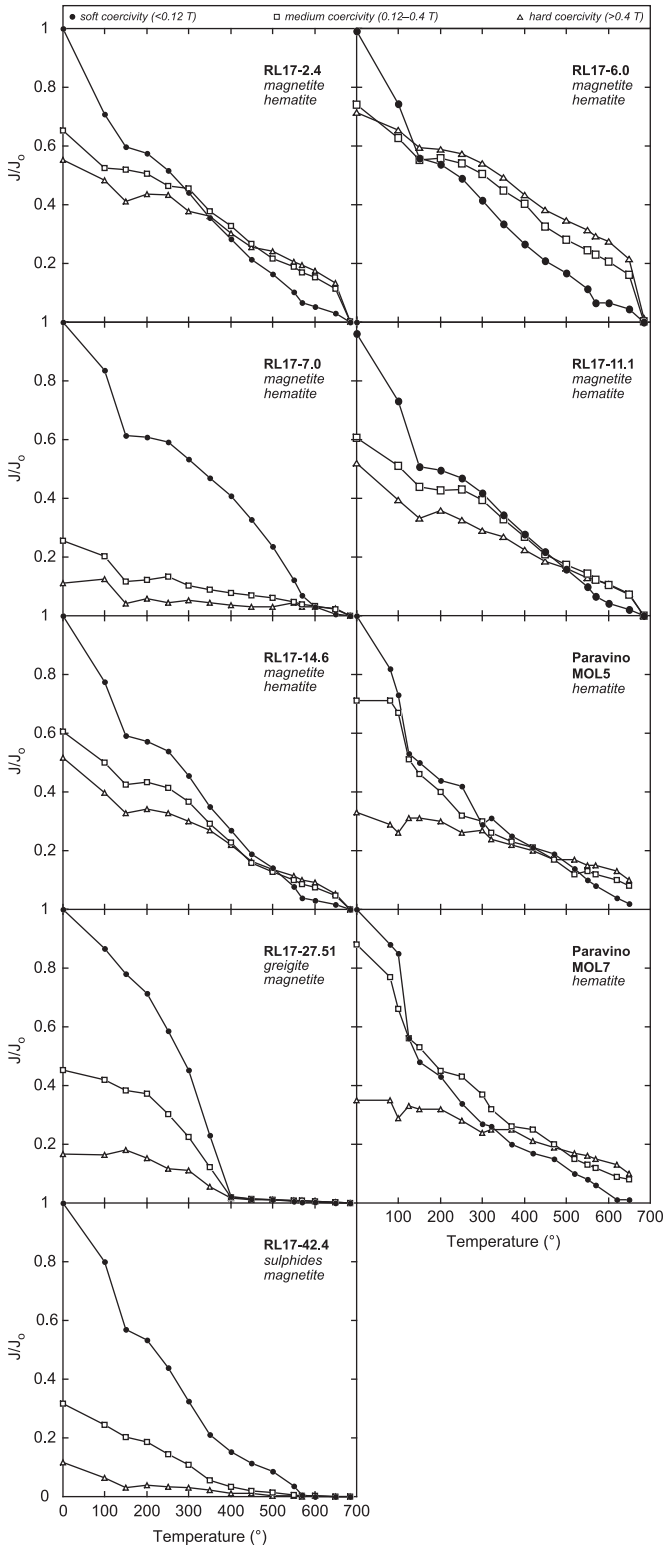

Fig. 5. Thermal decay of a three-component Isothermal remanent magnetization (IRM) on selected samples from core RL17 and the Paravino composite section. See text for discussion.

demagnetization data typically indicate the existence of an occasional low unblocking temperature A component usually superposed to a high unblocking temperature characteristic (ChRM) component (Fig. 6). The A component, removed between room temperature and less than ~250 °C, usually bears steep positive (down-pointing) inclinations, and is regarded as due to a normal polarity magnetization overprint probably induced by core drilling. The ChRM component was removed to the origin of the demagnetization axes mainly in the temperature range between ~150 °C and ~320 °C or occasionally ~570 °C in lacustrine Unit 4, and ~150 °C to a maximum of ~570 °C or occasionally ~680 °C in Units 5–8 (Fig. 2, panel 'unblocking T').

As core RL17 was not oriented with respect to the geographical north, only the inclination of the magnetic component vectors was used to interpret magnetic polarity stratigraphy. Inclination-only statistics of McFadden and Reid (1982) was performed on the ChRM component directions, yielding mean positive and negative inclinations of 51° ± 20° ($N = 11$; $k = 6.2$) and −46° ± 8° ($N = 29$; $k = 11.2$). These mean inclinations are somewhat shallower than the geocentric axial dipole (GAD) inclination of 64° for the core-site latitude, likely because of depositional inclination error or post-depositional compaction of the sediments (e.g., Tauxe, 2005).

In the Paravino composite section, orthogonal projections of thermal demagnetization data from oriented samples taken in the fine-grained sediments of the Molgora Conglomerate (Molinazzo sub-section; Fig. 3) indicate the existence of a low unblocking temperature A component usually superposed to a high unblocking temperature ChRM component (Fig. 6). The A component, removed between room temperature and less than ~200 °C, bears northerly-and-down directions, and is interpreted as a (sub)recent magnetization overprint of normal polarity. The ChRM component was removed in a few cases to the origin of the demagnetization axes mainly in the temperature range between ~250 and a maximum of ~680 °C (Fig. 3, panel 'unblocking T'; Fig. 6, sample MOL3); in other samples a linear component, not trending to the origin of the demagnetization axes, was isolated above ~250° to a maximum of 650 °C (Fig. 6, samples MOL1, MOL2, MOL6). The ChRM directions are highly scattered in declination, whereas the inclination values are consistently negative (overall mean Dec. = 186°, Inc. = −55°, $N = 5$, $k = 4.6$, $\alpha_{95} = 46.1°$), yielding negative virtual geomagnetic pole (VGP) latitudes comprised between −25° and −66° (Fig. 3).

The ChRM components from both core RL17 and the Paravino composite section are mainly regarded as acquired at or shortly after sediment deposition. The magnetization process is interpreted to be chiefly detrital (DRM or post-DRM). The presence of sulphides in lacustrine Unit 4 may suggest also a chemical contribution (CRM) to the total magnetization. In any case, this presumed CRM is interpreted to have been acquired at, or close to, the time of deposition, as no diagenetic features other than moderate degrees of compaction have been observed throughout the lacustrine sequence. Due to the strong weathering, deposits belonging to Unit 8 may display a later CRM overprint due to the formation of recent iron oxides in the vetusol. In core RL17, positive (negative) inclinations were acquired during normal (reverse) polarity of the Earth's magnetic field. In the Paravino composite section, scattered albeit exclusively negative VGP latitudes indicate remanence acquisition during a reverse polarity interval. We interpret the magnetic polarity stratigraphy using Berggren et al. (1995) time scale and taking into account the available pollen data from this study and the geoarcheological data of Cremaschi et al. (1990). In core RL17, the uppermost normal polarity magnetozone is ascribed to the Brunhes chron (<0.78 Ma) (Fig. 2), whereas the underlying reverse polarity magnetozone is interpreted as pertaining to the Matuyama chron. As the normal polarity Jaramillo subchron (1.07–0.99 Ma) was not recorded, the reverse polarity magnetozone found in core RL17 is attributed to the late Matuyama subchron (0.99–0.78 Ma). The Brunhes–Matuyama boundary (0.78 Ma) is not well defined as it falls between the upper part of the of coarse-grained sediments pertaining to Unit 5 and the overlying normal polarity deposits of Unit 6. In the Paravino composite section (Fig. 3), the reverse polarity magnetozone at the

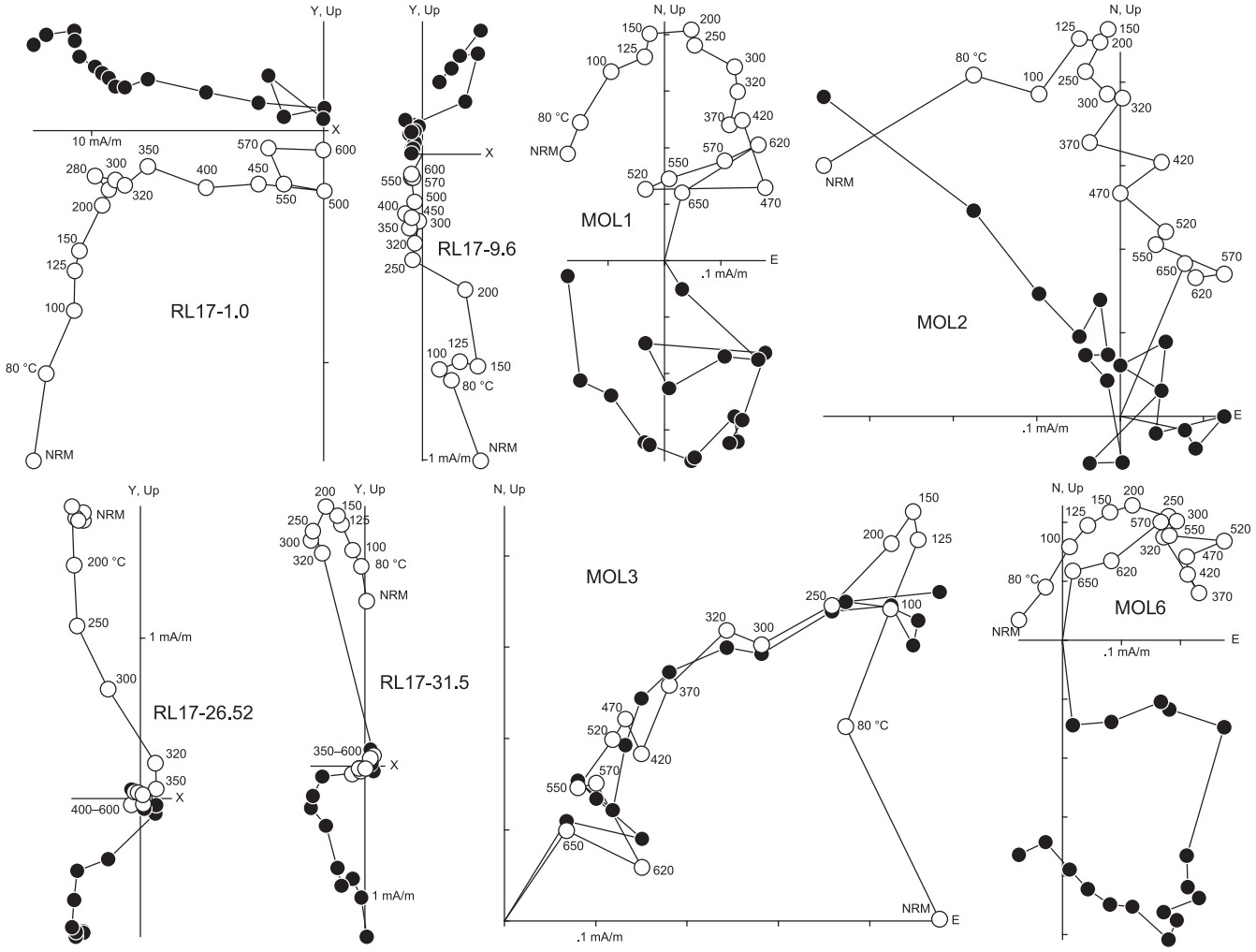

Fig. 6. Orthogonal projections of thermal demagnetization data of selected samples from core RL17 (left) and the Paravino composite section (right). Open (closed) symbols are projections onto the vertical (horizontal) plane. Horizontal projections in core RL17 samples have arbitrary azimuths, as cores were not oriented with respect to the geographic north.

base of the sequence is referred to the Matuyama chron, based on the pollen content.

6. Sand petrography

Quantitative petrography was studied on 18 mostly fine- to medium-grained sand samples collected from core RL17 and the Paravino composite section (Figs. 2, 3). Thin sections were prepared and stained with alizarin-red to distinguish dolomite from calcite. In each sample, 400 points were counted according to the Gazzi-Dickinson method (Ingersoll et al., 1984; Zuffa, 1985). A detailed petrological classification scheme, including heavy minerals, was used for quantitative estimates of the coarse-grained rock fraction (Table B1 in Appendix B). Metamorphic grains were classified according to the protolith composition and metamorphic rank. Average rank for each sample was expressed by the metamorphic index (MI), which varies from 0 in detritus from sedimentary and volcanic cover rocks to 500 in detritus from high-grade basement rocks (Garzanti and Vezzoli, 2003). Similarity analysis was performed in order to quantitatively discriminate sediment provenance. Sediment provenance was interpreted by means of the statistical comparison with the Alpine petrographical database (Garzanti et al., 2006), based on actualistic sand petrofacies. The similarity analysis was carried out by comparing detrital modes of modern and ancient sands with a linear mixing model (Weltje, 1997). The best modern analogues of ancient sedimentary deposits were identified by statistical analysis using the multiple correlation index R of Vezzoli and Garzanti (2009) (i.e., the end-member corresponding to *R* closest to 1). The similarity analysis was performed by using R-package compositions (van den Boogaart and Tolosana-Delgado, 2008), applied to the additive log ratio transformed data (Aitchison, 1986).

In core RL17, four distinct petrofacies have been recognized from base to top (Fig. 2; Table B2 in Appendix B).

Petrofacies B1, represented by the sample at 45.6 m, pertaining to the Bergamo Flysch (Curone Valley bedrock) and characterized by quartz, dolostone, and limestone grains, as well as mica and feldspars with subordinate metasedimentary and volcanic rock fragments. Heavy minerals are negligible.

Petrofacies B2, subdivided in two sub-petrofacies – B2a and B2b – that are similar in composition but are kept separate because distributed throughout distinct stratigraphic intervals (Fig. 2). Sub-petrofacies B2a is represented by samples at 41.0 and 41.3 m, whereas the sub-petrofacies B2b is represented by the sample at 7.8 m. Both sub-petrofacies consist of abundant quartzose sands with few feldspars (mainly K-feldspars), felsitic volcanic grains, and chert, associated with rare heavy minerals such as tourmaline. This petrographical signature is not referable to any known detrital signature of modern Alpine rivers. The great amount of stable and ultra-stable minerals

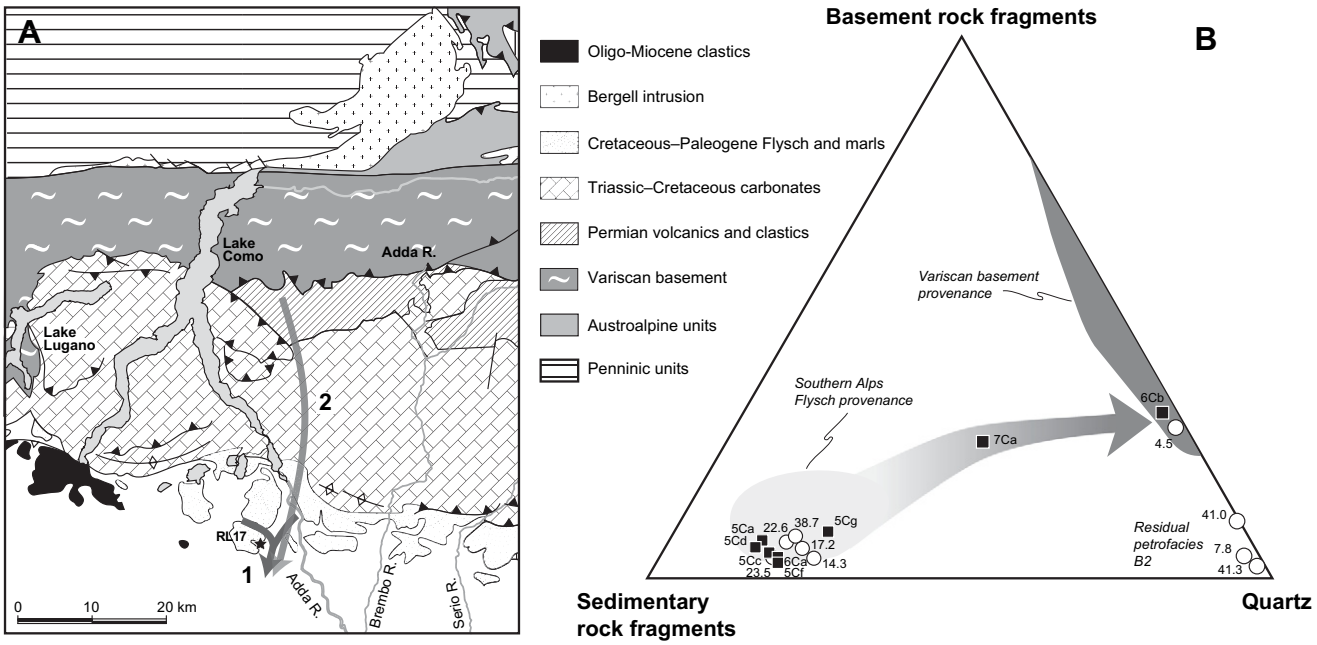

Fig. 7. (A) Simplified lithologic map of the Southern Alps with arrows indicating the provenance of Molgora Conglomerate (1) and Bozzente Allogroup gravels (2), as deduced from the respective petrographic composition. (B) Ternary diagram showing the petrographic composition of sediments from Bagaggera core RL17 and the Paravino composite section (see Table B2 in Appendix B for individual sample composition). The ternary diagram shows basement rock fragments (metapsammite/metafelsite rock fragments with staurolite), sedimentary rock fragments (limestone, dolostone, shale and siltstone), and quartz. Shaded areas (95% confidence regions about the mean; Weltje, 2002) indicate modern detrital signatures of Cretaceous Flysch and the Variscan basement of the Southern Alps (modified after Garzanti et al., 2006).

(e.g., quartz and tourmaline) and the scarce presence of lower stability minerals (e.g., feldspars) seem to indicate a residual nature for these sediments, probably derived from the local erosion of well-developed paleosols (see also Cremaschi et al., 1985).

Petrofacies B3, represented by samples at 14.3, 17.2, 22.6, 23.5, and 38.7 m, characterized by carbonate (limestone and dolostone) grains, quartz, and sandstone rock fragments with calcitic cement; heavy minerals are negligible. This petrographical composition well compares to the detrital signature of the modern Brembo River (Fig. 7), indicating sediment provenance from the Mesozoic sedimentary cover of the Southern Alps ($R = 80\%$; Fig. 7).

Petrofacies B4, represented by the sample at 4.5 m characterized by quartz with minor felsic volcanic grains, metapsammite/metafelsite rock fragments (with sillimanite and garnet), and feldspars; heavy minerals include garnet and staurolite. High-grade metamorphic grains associated with staurolite and garnet point to a sediment provenance from the Variscan metamorphic basement of the Southern Alps ($R = 75\%$; Fig. 7).

In the Paravino composite section (Fig. 3; Table B2 in Appendix B), two distinct petrofacies have been recognized, from base to top.

Petrofacies P1, represented by samples 5Ca, 5Cc, 5Cd, 5Cf, 5Cg and 6Ca, which are rather uniform in composition and consist of calcareous grains (oolitic grainstones, grains with sponge spicules and calcispheres) and sandstone rock fragments with calcitic cement. A few felsic volcanic grains, chert grains (with radiolarians and sponge spicules), and gneissic rock fragments have also been found, whereas heavy minerals are absent. Sample 5Cg records the first appearance of sparse felsic volcanic grains. This petrographical composition well compares to the detrital signature of the modern Brembo River, indicating sediment provenance from the Mesozoic sedimentary cover of the Southern Alps ($R = 75\%$; Fig. 7).

Petrofacies P2, represented by samples 6Cb and 7Ca. Sample 6Cb consists of quartzose sand, and includes metapsammite/metafelsite rock fragments (with sillimanite and staurolite), felsic volcanic grains, and feldspars. Sample 7Ca is characterized by the presence of felsic volcanic grains, gneissic rock fragments with garnet, amphibolite rock fragments, and a few staurolite grains. Heavy minerals are few and include staurolite and garnet. Similarity analysis shows that the detrital signature of these sediments is compatible with a provenance from the Variscan metamorphic basement of the Southern Alps ($R = 78\%$; Fig. 7).

Similarity analysis indicates that petrofacies B3 of core RL17 well compares with petrofacies P1 of the Paravino section ($R = 80\%$; Fig. 7). Samples from these correlative intervals show similar calcareous grains and rock fragments with calcitic cement. Detrital modes of sample from petrofacies B4 of core RL17 well compare with those from petrofacies P2 of the Paravino section ($R = 90\%$; Fig. 7). Felsic volcanic grains and high-grade gneisses, associated with staurolite and garnet, indicate provenance from the Variscan metamorphic basement in both petrofacies (Fig. 7). These data basically agree with the petrographical data previously obtained by Cremaschi et al. (1985) on heavy minerals from outcrop sections.

7. Evolution of the Bagaggera basin

The interdisciplinary study on the Bagaggera RL17 core and the Paravino composite section allows reconstructing the overall Pleistocene evolution of the Bagaggera basin and the surrounding area (Fig. 8). After a phase of chaotic slope deposition (Unit 3; Fig. 2), the ~25-m-thick Bagaggera lacustrine sequence (Unit 4; Fig. 2) developed during the late Matuyama subchron (0.99–0.78 Ma). According to the pollen record (Zone BA1), this ~25-m-thick lacustrine sequence deposited during a unique cold phase, ascribable to a single even Marine Isotope Stage (MIS) (Lisiecki and Raymo, 2005), in agreement with the former interpretation of Venzo (1948, 1952).

The onset of major Pleistocene glaciations in the Southern Alps is currently dated to MIS 22 at ~0.87 Ma within the late Matuyama subchron (Muttoni et al., 2003, 2007). Hence, the damming of the Curone Valley at Bagaggera likely occurred during MIS 22. The absence of dropstones or coarse-grained debris lenses (Eyles and Menzies, 1983; Thomas and Connell, 1985) seems to exclude the

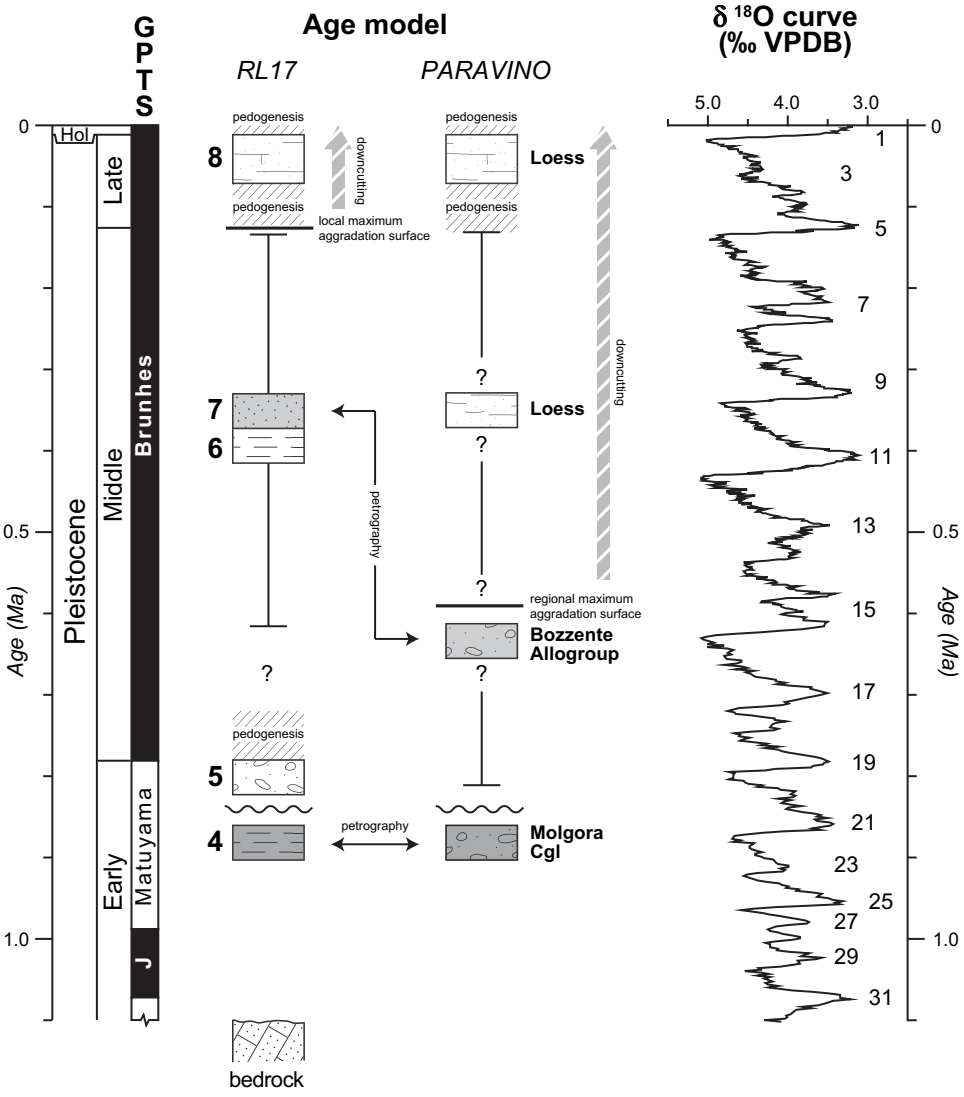

Fig. 8. Chronostratigraphic scheme showing the correlation between core RL17 and the Paravino composite section. The LR04 benthic $\delta^{18}O$ stack (Lisiecki and Raymo, 2005) is reported with indication of odd (i.e. interglacial) Marine Isotope Stages (MIS). The Geomagnetic Polarity Time Scale (GPTS) is from Berggren et al. (1995).

possibility of damming by direct glacier contact. From field geology (Fig. 1), it follows that the damming was due to the deposition of a fluvial body, in agreement with Orombelli (1979). Petrographical data show a common sediment provenance for the Bagaggera lacustrine sequence and the Molgora Conglomerate, which, coupled with the available age constraints provided by magnetostratigraphy and pollen analysis, suggest a direct link between the deposition of the Molgora Conglomerate and the formation of lake Bagaggera (Fig. 8). Lacustrine sedimentation ended with an erosional phase, which likely occurred during interglacial MIS 21. Next, the deposition of alluvial fan gravels of local (intra-valley) provenance (Unit 5; Fig. 2) shortly before the Brunhes–Matuyama boundary is referred to a new phase of gravel progradation possibly occurred during glacial MIS 20. Then, swamp to lacustrine sediments (Unit 6; Fig. 2) were deposited under warm-temperate climate conditions (pollen zones BA2 and BA3). Magnetostratigraphy and pollen content allow to constrain these swamp-lacustrine deposits to an interglacial stage of the Brunhes chron (<0.78 Ma), possibly comprised between MIS 15 and MIS 7 (~0.6–0.18 Ma). The basin was then filled by fluvial sands (Unit 7; Fig. 2), which, according to petrographical data, originated, together with the gravels of the Bozzente Allogroup (Fig. 3), from the Variscan metamorphic basement of the Southern Alps (Fig. 7) during a Middle Pleistocene glacial phase.

Taken as a whole, the petrographical data in the study area point to a paleodrainage evolution from a local catchment area limited to the Southern Alps foothills (Molgora Conglomerate) to a larger catchment area extending as far north as the Variscan basement of the Southern Alps (Unit 7 and Bozzente Allogroup). This important change, already observed by Orombelli and Gnaccolini (1978), is now bio-magnetostratigraphically constrained to the time interval between the late Matuyama subchron and the early Brunhes chron and it is possibly referred to the effects of glacial activity in the mountain area upstream the Bagaggera basin. To this regard, remarkable is the absence of Central Alps lithotypes (e.g. serpentinites or Bergell intrusives) in the Bozzente Allogroup gravels and in Unit 7 sands, suggesting that the glaciers developed in the mountain area upstream the Bagaggera basin were probably not connected with the Central Alps until the late Middle Pleistocene.

Finally, above Unit 7, only reworked loess deposited in the Bagaggera basin since MIS 4, as inferred from the TL dating of 60.5 ± 7.5 ka on a burnt flint found at the base of the loess succession (Cremaschi et al., 1990). These uppermost deposits suggest that the

Bagaggera area remained morphologically isolated by the Curone Valley fluvial dynamics, becoming a loess basin locally influenced by slope processes. Since then on, sediment accumulation rates strongly decreased, weathering processes prevailed, and a ~8-m-thick vetusol developed at the top of the succession.

8. Climate-driven sedimentation in northern Italy and the Alps during the late Matuyama

Our findings on the evolution of the Bagaggera basin are in agreement with similar scenarios of climate-driven changes in style of deposition occurring during the late Matuyama subchron in different orographic (intermountain *vs.* foreland basins) and geodynamic settings (Po Plain *vs.* Venetian Plain) of the greater Alpine–Po Plain area, as illustrated hereafter.

During the Early Pleistocene Jaramillo subchron (1.07–0.99 Ma), a first moderate climate-driven alluvial fan progradation triggered lacustrine basins formation at the Southern Alps margin by alluvial damming of lateral drainage systems (e.g. the Ranica sequence; Ravazzi et al., 2005), whereas, more basinward in the Po basin, fan-delta progradation occurred (Scardia et al., 2006). Nonetheless, valley glaciers reached the Po Plain only during the late Matuyama subchron, as testified by the reverse polarity magnetization of (glacio)lacustrine deposits associated with the early stages of building of the Ivrea (Carraro et al., 1991), Iseo (core

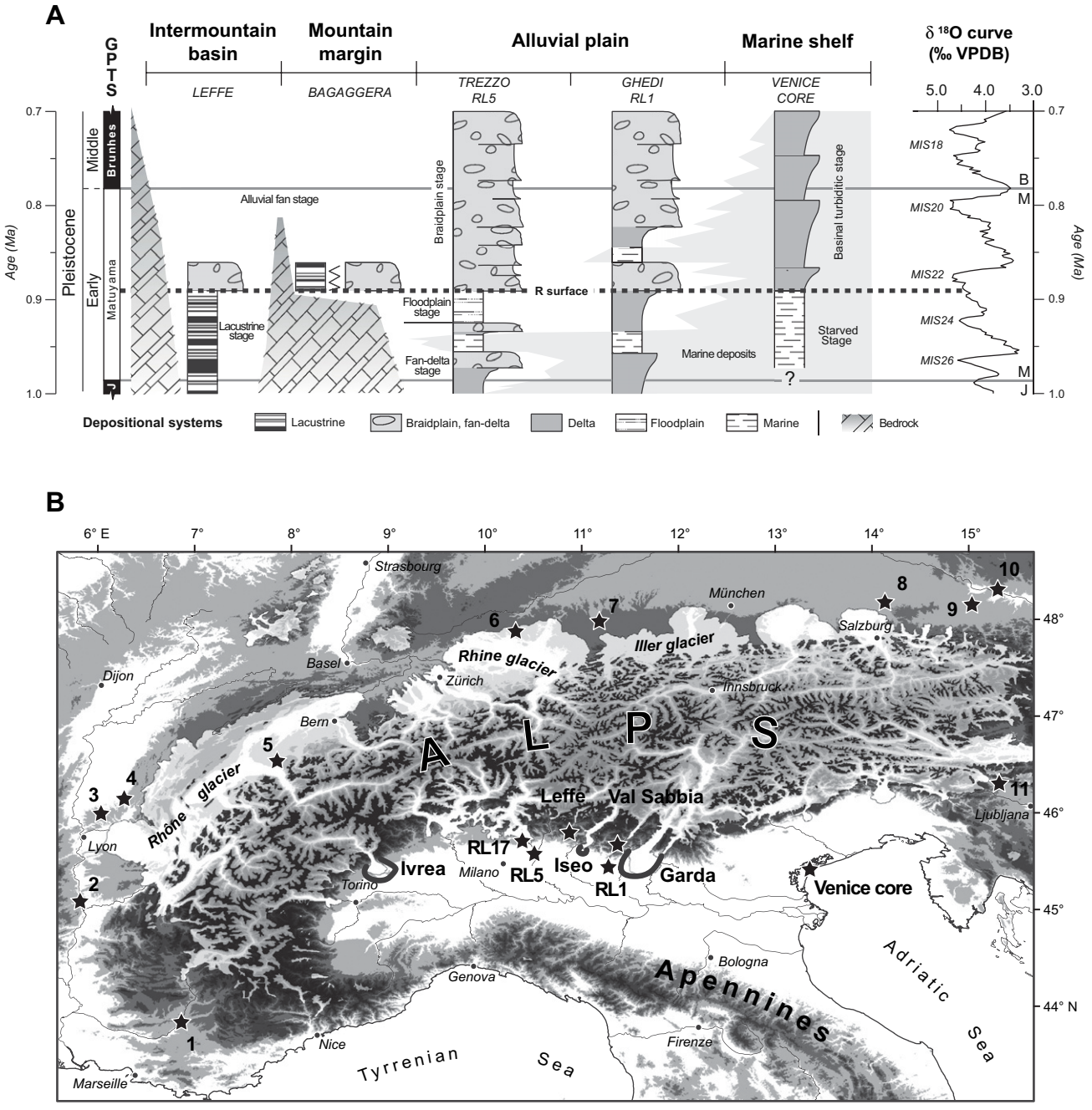

Fig. 9. Correlation of stratigraphic data across the Southern Alps–Po Plain system (A) and location of the sites discussed in the text (B). The intensification of glacial activity during the late Matuyama subchron triggered the onset of high-energy sedimentation in different orographic and geodynamic settings of the Southern Alps–Po Plain system and the greater Alpine area. Stratigraphic data are from Muttoni et al. (2007), Scardia et al. (2006), Kent et al. (2002), and this study. The Geomagnetic Polarity Time Scale (GPTS) is from Berggren et al. (1995). In panel B, the extension of the Last Glacial Maximum (Elhers and Gibbard, 2004) is displayed in white. See text for discussion.

Cremignane RL6; Scardia et al., 2006), and Garda (Cremaschi, 1987) morainic amphitheatres (Fig. 9b). At broadly the same time, in intermountain basins of the Southern Alps (e.g., Leffe basin; Fig. 9b), massive alluvial fan progradation (e.g., Casnigo Unit) terminated at MIS 22 times a long history of Early Pleistocene lacustrine sedimentation by basin overfilling (Fig. 9a) (Muttoni et al., 2007). A similar evolution can be likely recognized also in the nearby Val Sabbia intermountain basin (Fig. 9b), where Early Pleistocene travertine and fine-grained deposits pass to high-energy Middle Pleistocene conglomerates (Chardon, 1975; Baroni et al., 1988). At the Southern Alps margin, strongly prograding and aggrading alluvial fan bodies dammed lateral valleys, as documented by the Bagaggera sequence in the Curone Valley (Fig. 9a). More distally in the Po Plain (e.g. cores Trezzo RL5 and Ghedi RL1; Fig. 9a), building of glacial amphitheatres and alluvial fan progradation are regionally recorded by a major shift from mainly meandering to exclusively braided fluvial systems dated in several cores to MIS 22 by means of magnetostratigraphy (Muttoni et al., 2003; Scardia et al., 2006). More eastward in the Adriatic Sea, this regional shift in style of deposition seems to correlate to the progradation of basinal turbidites onto a previously starved slope setting, occurring (shortly) before the Brunhes–Matuyama boundary (Venice core; Kent et al., 2002; Massari et al., 2004; Fig. 9a).

Elsewhere in the Alps, the Early Pleistocene sedimentary history seems to be less well documented and constrained in time, with some notable exceptions. In France, Dubar and Semah (1986) reported the magnetostratigraphy of a composite section from the middle Durance Valley (Fig. 9b, site 1), where Günz gravel deposits pass in stratigraphic continuity to reverse polarity (late Matuyama) interglacial swamp deposits with *Carya* and *Tsuga*, covered by normal polarity (early Brunhes) loess deposits. Reverse magnetic polarity is furthermore reported in loess layers covering the Crozes–Hermitage fluvioglacial deposits (Fig. 9b, site 2; Mandier, 1984, in Billard and Orombelli, 1986), in the la Chapelle-du-Chatelard deposits of the Les Dombes glacial complex (Rhône Glacier area; Fig. 9b, site 3; Billard and Orombelli, 1986), and in the lowermost fluvial deposits of the Les Rippes terrace (Fig. 9b, site 4; Billard and Orombelli, 1986), albeit no paleomagnetic data have been illustrated or discussed.

In the Swiss Alpine foreland, the development of a cold (glaciolacustrine) lake during the late Matuyama subchron is testified at Ecoteaux (Rhône Glacier area; Fig. 9b, site 5), Here, on the basis of an integrated bio-magnetostratigraphic study of a 75-m-deep core, Pugin et al. (1993) report evidence for a lodgement till overlain by a palynologically cold lacustrine sequence deposited during a reverse magnetic polarity interval, ascribed to the Matuyama chron. These Matuyama lacustrine deposits are in turn unconformably overlain by a younger lacustrine succession spanning a glacial–interglacial cycle and displaying normal magnetic polarity, referred to the Brunhes chron (Pugin et al., 1993). The pollen record from the Brunhes lacustrine sequence supports the attribution to a Middle Pleistocene interglacial, possibly MIS 19, 17, or 15 (Bézat, 2008).

In southern Germany at Heiligenberg, Höchsten, and Zeil (Rhine glacier area; Fig. 9b, site 6), reverse magnetic polarity is consistently documented in fine-grained layers belonging to Günz gravel deposits (Bibus et al., 1996). More eastwards, at Memmingen (Iller Glacier area; Fig. 9, site 7), Günz and Mindel Deckenschotter gravels were recently dated by means of cosmogenic ^{26}Al and ^{10}Be burial technique to 2.35 Ma (+1.08/−0.88) and 0.68 Ma (+0.23/−0.24), respectively (Häuselmann et al., 2007), with the younger age (0.68 Ma) consistent, within error limits, with MIS 22–MIS 12 (0.87–0.44 Ma), whereas the older age (2.35 Ma), with errors of up to 40%, clearly needs refinements.

In Austria, paleomagnetic investigations on sites from Günz moraines (Mauerkirchen; Fig. 9b, site 8) as well as from the Älterer Deckenschotter (Würzburger and Linz; Fig. 9b, sites 9 and 10) provided thus far evidence of exclusive normal magnetic polarity (Fink, 1979), possibly pertaining to the Brunhes chron. Finally, in Slovenia, Günz gravel deposits from the upper Sara Valley could be referred to the Matuyama chron on the basis of paleomagnetic and cosmogenic ^{10}Be analyses (Fig. 9b, site 11; Pavich and Vidic, 1993).

From the above, it is evident that the Günz deposits in France, Switzerland, southern Germany, and Slovenia (reverse polarity) are not isochronous with the Günz deposits in Austria (normal polarity), and that the surviving practice of identifying Pleistocene deposits using the classic Penck and Brückner (1909) nomenclature for pre-Würm glaciations (Günz, Mindel, and Riss) can be misleading in terms of chronostratigraphy (Šibrava, 1986).

A plausible explanation for all these events recorded throughout the entire Alpine area in close temporal contiguity – during the late Matuyama subchron – rises from taking into consideration global climate teleconnections. Until the Jaramillo subchron, long warm-temperate stages bracketing cooler phases of usually short duration prevailed. No substantial valley glaciers were formed in the Alpine area, and the Southern Alps margin remained partially forested (Muttoni et al., 2007). A major shift toward major glacial cycles occurred during the late Matuyama subchron, starting with MIS 22 and continuing during the ensuing Brunhes chron (Shackleton, 1995; Lisiecki and Raymo, 2005). Pleistocene glacial stages such as MIS 22 were characterized by enhanced glaciers development and glacio-eustatic lowstands, as well as forest withdrawal in the Alpine region. Long phases of persistent low forest cover (steppe-forest at low altitudes), coupled with marked base level glacio-eustatic falls, promoted physical erosion and the progradation of alluvial fans from the Alps toward the peripheral plains. Here, sediments were redistributed by braided river systems and ended up in the northern Adriatic Sea as basinal turbidites, as observed in the Venice subsurface (Kent et al., 2002; Massari et al., 2004).

In this scenario of climatic forcing on sedimentation, the oldest (reverse polarity) episodes pointing to a major expansion of the Alpine valley glaciers (e.g., Rhône, Ivrea, Iseo, Garda), may date back to the late Matuyama subchron and were likely synchronous with the alluvial fan and braidplain progradation observed in the southern foreland of the Alps (e.g. Molgora Conglomerate of this study, Casnigo unit at Leffe) and the deposition of most of the so-called Günz and Älterer Deckenschotter (reverse polarity) deposits in the western, northern, and eastern forelands of the Alps.

9. Conclusions

Ancient lacustrine basins are remarkable repositories of stratigraphic events in otherwise usually fragmented continental realms. By applying a multidisciplinary approach to the study of a long core and nearby land exposures, we were able to date a lacustrine sequence (lake Bagaggera) and link it to a virtually undatable conglomeratic succession (Molgora Conglomerate) in a cause–effect relationship. We found that lake Bagaggera, previously referred to a generic pre-glacial Early Pleistocene (Bucha and Šibrava, 1977; Billard et al., 1983; Cremaschi et al., 1985), formed during a cold, mostly treeless phase as the result of damming of the Curone Valley by the prograding fan of the Molgora Conglomerate. This event occurred during the late Matuyama subchron (0.99–0.78 Ma), probably at glacial MIS 22 (~0.87 Ma). These new data are consistent with the regional late Early Pleistocene scenario of climate forcing on sedimentation depicted for the Alps–Po Plain system (Muttoni et al., 2003, 2007) and with similar events occurring in the same time span in different orographic and geodynamic settings of the greater Alpine area.

The first major Pleistocene radial expansion of the Alpine valley glaciers (e.g., Rhône, Ivrea, Iseo, Garda) probably occurred during the late Matuyama subchron and is also documented by the coeval progradation of alluvial fans and, more generally, high-energy fluvial systems from the Alps to all the adjoining foreland basins.

Acknowledgments

This research was generated in the frame of a collaboration project between Regione Lombardia, IREALP, C.N.R.-IDPA, and the Montevecchia and Curone Valley Park. A. Bolis, M. Cereda, G. Galimberti, R. Laffi, A. Piccin, P.M. Rossi, and D. Sciunnach are thanked for support and collaboration. This study strongly benefited from the scientific suggestions and contributions of S. Andò, D. Gianolla, E. Martinetto, L. Pacifico, R. Pini, and F. Tremolada. We thank A. Bini, F. Tomasi, and L. Zuccoli for the extensive support during the early stages of this project. We also thank P. Gibbard and an anonymous referee for their constructive reviews, criticism and comments.

Appendix A

Core Bagaggera RL17 (Fig. 2)

Core description and facies analysis has been performed by taking into account sediment texture, structure, and colour, vertical lithofacies variations, and the occurrence of accessory materials, including roots, organic matter, wood fragments, bioturbation, and weathering. Texture and colour were determined by means of a 0.5 ϕ sediment comparator (Udden-Wentworth grain-size classification scheme; Wentworth, 1922) and the Munsell Soil Colour Chart, respectively. $CaCO_3$ content was evaluated with 5% HCl solution.

Unit 1 (46.80–45.10m). *Description:* hybrid arenite with abundant quartz and mica, and dip of ~70°. *Interpretation:* Bergamo Flysch (Campanian; Gelati and Passeri, 1967; Galbiati, 1969; Bersezio and Fornaciari, 1994).

Unit 2 (45.10–44.30m). *Description:* medium- to very coarse-grained, quartzose–micaceous, massive pebbly sand. *Interpretation:* physical weathering of the Bergamo Flysch.

Unit 3 (44.30–41.90m). *Description:* chaotic package of monogenic coarse-grained quartzose–micaceous sand and Bergamo Flysch pebbles, with sparse coalified wood fragments. *Colour:* 5B 7/1. *Interpretation:* slope deposit.

Unit 4 (41.90–17.30m). *Description:* coarse- to fine-grained, organic-rich sands with plant remains, arranged in a unique, thick, fining-upward sequence, passing upward to a monotonous cm-thick horizontally laminated silty clay succession with interbedded very fine- to fine-grained sand layers. Sand layers are generally normal graded with a sharp base. *Colour:* 10Y 3/1, 5GY 6/1, 10GY 6/1, 5Y 3/2 (basal organic-rich sand) and 5 PB 6/1 (silty clay). *Interpretation:* at the whole Unit 4 may be interpreted as a transgressive to deepening upward lacustrine sequence, consisting of near-shore/transgressive organic-rich deposits passing upward to basinal detrital deposits. Laminated silty clay, normal graded sands and the vertical persistence of the lithofacies point to a lacustrine basinal environment with turbidites and high sedimentation rates, deduced by the cm-thick lamination, low pollen concentration, and rather uniform magnetic susceptibility values. The complete lacking of dropped debris or isolated, coarse-grained debris lenses, and the presence of a vegetational cover in the surroundings testified by the pollen record likely do not support a subglacial or proglacial lacustrine environment (Eyles and Menzies, 1983; Thomas and Connell, 1985; Moscariello et al., 2000).

Unit 5 (17.30–11.15m). *Description:* vertical stacking of silt to gravel coarsening-upward cycles, locally weathered and bounded by erosional surfaces. The lower boundary of the unit is a high-angle, erosional surface, carved in the underlying Unit 4. Pebbles and cobbles are sub-rounded and consist of marly limestones, quartzose–micaceous arenites, and cherts; sparse mud clasts are observed. *Colour:* 2.5Y 7/3, 2.5Y 6/4, 5 PB 6/1, 10YR 6/8. *Interpretation:* Unit 5 can be interpreted as a prograding alluvial fan with an intra-valley provenance, deduced by gravel and sand petrography. Colour variations and local weathered layers may have been produced by groundwater level fluctuations.

Unit 6 (11.15–4.70m). *Description:* clay to medium-grained silty sand coarsening-upward cycles passing upward to laminated silty clay, with organic-rich layer, bioturbation, and sparse carbonized wood fragments. Hydromorphic features strongly affect the base of the deposit. *Colour:* 5G 6/1, 5 PB 5/1, 5 PB 7/1 (basal coarsening-upward cycles) and 2.5Y 7/4 (silty clay). *Interpretation:* swamp to lacustrine sequence, based on pollen content and the hydromorphic features.

Unit 7 (4.70–2.50m). *Description:* strongly weathered very fine- to medium-grained sand with silty matrix and sparse granules. *Colour:* 10YR 6/6, 10YR 7/6. *Interpretation:* fluvial deposit with extra-valley provenance, deduced by sand petrography.

Unit 8 (2.50–0.30m). *Description:* strongly weathered stacking of loam, locally sandy, with sparse quartz and chert granules and a very fine-grained gravel layer. Fe–Mn nodules horizons are observed. *Colour:* 10YR 7/8, 7.5 YR 5/6 (background) and 5YR 5/8 (mottling). *Interpretation:* one or, more likely, two water-reworked loess layers. The 60.5 ± 7.5 ka TL age provided by Cremaschi et al. (1990) can referred to the base of Unit 2.

Unit 9 (0.30–0m). Layer consisting of reworked material with brick fragments. The uppermost section of the core (Units 6–8) is strongly weathered in a vetusol (Cremaschi et al., 1985; Cremaschi, 1987) with decalcification and oxidation front at ~7 m and ~8 m, respectively.

Paravino composite section (Fig. 3)

This section is composed by three different sub-sections, located in Fig. 1 and described according to Miall's fluvial lithofacies classification scheme (Miall, 2006).

Molinazzo sub-section (Fig. 1, outcrop A). The exposed section was extended downward with a hand drill to the depth of 1.8 m from the Curone River bed. At the base of the section (28.8–26 m; Fig. 3) there are interlaminations of silt, mud and fine- to medium-grained laminated (ripple and horizontal lamination) sand and sandstone (lithofacies *Fl*), with molluscs fragments and an operculum of *Bythinia* cf. *B. tentaculata* (L.) (D. Giannolla, written comm. 2008). Sand petrographic composition belongs to the petrofacies P1 (Fig. 3). Upward (26–21 m; Fig. 3), with an erosional undulated boundary, there is a stack of clast- to matrix-supported, massive or crudely-bedded, coarse-grained conglomerates (lithofacies *Gmm*, *Gcm*, *Gh*) with rare sandstone layers (lithofacies *Sh*, *Sm*).

Molgora River sub-section (Fig. 1, outcrop B). The outcrop (21–11 m; Fig. 3) shows a vertical succession of clast-supported, coarse-grained conglomerates referred to the Molgora Conglomerate, bearing horizontal and planar crossbeds stratification (lithofacies *Gcm*, *Gh*, *Gp*), local openwork texture, with petrofacies P1. Upward, deep weathering pits intercalated to conglomerate pinnacles (the so-called "geologische Orgeln") are partially observed.

Paravino sub-section (Fig. 1, outcrop C). At the base (11–8.8 m; Fig. 3), the outcrop shows clast-supported, massive, coarse-grained conglomerate (lithofacies *Gcm*) with petrofacies P1, upward weathered and shaped into a pinnacle ("geologische Orgeln"). Next (8.8–1.8 m; Fig. 3) is a massive, strongly weathered, coarse-grained gravel, with petrofacies P2. At the top (1.8–0 m; Fig. 3) there are weathered clayey silt layers, interpreted as loess by Cremaschi (1987) and Strini (2001).

On the whole, the fluvial conglomerate, ascribed to the Molgora Conglomerate (Strini, 2001; Bini et al., 2004), is dominated by

lithofacies *Gmm*, *Gcm*, *Gh* with subordinate lithofacies *Gp*, *Sh*, *Sm* and, very rarely, *Fl*; clasts are sub-rounded to rounded, locally embricated, and may reach a 0.5 m size. Orombelli (1979) reported the occurrence of clasts exceeding the 1 m size in an artificial cut at Pagnano (Fig. 1). Lithofacies association mostly points to a fluvial environment dominated by sediment gravity flows, gravel bars and bed forms, ascribable to an alluvial fan or a very proximal braidplain (Blair and McPherson, 1994; Miall, 2006). The upper weathered gravels have been ascribed to the Bozzente Allogroup by Strini (2001) and Bini et al. (2004), and their sedimentologic features are mostly obliterated. The presence of sub-rounded to rounded clasts up to 0.4 m size may allow to interpret the Bozzente Allogroup as a proximal braidplain deposit.

Appendix B

Table B1
Recalculated key indices for framework composition.

Key Indices	Definition
Bulk Composition[a]	
Q	quartz
KF	K-feldspar
P	plagioclase
Lvf	felsic volcanic and subvolcanic lithic grains
Lvm	andesitic and mafic volcanic and subvolcanic lithic grains
Lcc	limestone grains
Lcd	dolostone grains
Lp	terrigenous lithic grains (shale, siltstone)
Lch	chert lithic grains
Lms	metasedimentary lithic grains (very-low to low rank)
Lmv	metavolcanic lithic grains (very-low to low rank)
Lmf	metapelite/metapsammite and metafelsite lithic grains (medium to high rank)
Lmb	metabasite lithic grains (medium to high rank)
Lu	ultramafic lithic grains (serpentinite, foliated serpentineschist)
Mu	muscovite
Bi	biotite
AP	amphiboles and pyroxenes
&HM	other heavy minerals
MI	Metamorphic Index by Garzanti and Vezzoli (2003)

[a] Primary parameters calculated with the Gazzi-Dickinson method.

References

Aitchison, J., 1986. The Statistical Analysis of Compositional Data. Chapman Hall, London.

Baroni, C., Cremaschi, M., Jadoul, F., Quinif, Y., 1988. Significato stratigrafico e paleopedologico delle datazioni U/Th relative al cemento del conglomerato di sotto castello (Val Sabbia, Brescia). Natura Bresciana 24, 259–267.

Berggren, W.A., Hilgen, F.J., Langereis, C.G., Kent, D.V., Obradovich, J.D., Raffi, I., Raymo, M.E., Shackleton, N.J., 1995. Late Neogene chronology: new perspectives in high-resolution stratigraphy. Geological Society of America Bulletin 107, 1272–1287.

Bersezio, R., Fornaciari, M., 1994. Syntectonic upper cretaceous deep-water sequences of Lombardy basin (southern Alps, northern Italy). Eclogae Geologicae Helvetiae 87, 833–862.

Beug, H.J., 2004. Leitfaden der Pollenbestimmung für Mitteleuropa und angrenzende Gebiete. Verlag Friedrich Pfeil, Munich.

Bibus, E., Bludau, W., Ellwanger, D., Fromm, K., Kösel, M., Schreiner, A., 1996. On prewürm glacial and interglacial deposits of the Rhine glacier (South German Alpine foreland, upper Swabia, Baden-Württemberg). In: Turner, C. (Ed.), The Early Middle Pleistocene in Europe. Balkema, Rotterdam, pp. 195–204.

Billard, A., Orombelli, G., 1986. Quaternary glaciations in the French and Italian piedmonts of the Alps. Quaternary Science Reviews 5, 407–411.

Billard, A., Bucha, V., Horacek, J., Orombelli, G., 1983. Preliminary paleomagnetic investigations on Pleistocene sequences in Lombardy, Northern Italy. Rivista Italiana di Paleontologia e Stratigrafia 88, 295–318.

Bini, A., Strini, A., Violanti, D., Zuccoli, L., 2004. Geologia di sottosuolo nell'alta pianura a NE di Milano. Il Quaternario 17, 343–354.

Blair, T.C., McPherson, J.G., 1994. Alluvial fans and their natural distinction from rivers based on morphology, hydraulic processes, sedimentary processes, and facies assemblages. Journal of Sedimentary Research 64, 450–489.

van den Boogaart, K.G., Tolosana-Delgado, R., 2008. "Compositions": a unified R package to analyze compositional data. Computers and Geosciences 34, 320–338.

Bucha, V., Šibrava, V., 1977. On the correlation of quaternary stratigraphy stages in the Northern Hemisphere. In: IGCP Project 73/1/24. Quaternary Glaciations in the Northern Hemisphere 4, 91–101.

Bézat E., 2008. Contribution pollinique à l'étude du Pléistocène de la région lémanique (Suisse). PhD thesis, University of Lausanne.

Carraro, F., Lanza, R., Perotto, A., Zanella, E., 1991. L'evoluzione morfologica del Biellese occidentale durante il Peistocene inferiore e medio, in relazione all'inizio della costruzione dell'Anfiteatro Morenico d'Ivrea. Bollettino del Museo Regionale di Scienze Naturali di Torino 9 (Suppl. 1), 99–117.

Chardon, M., 1975. Les Préalpes Lombardes et leur bordures. Librairie H. Champion, Paris.

Cremaschi, M., 1987. Paleosols and Vetusols in the Central Po Plain (Northern Italy). Unicopli, Milan.

Cremaschi, M., Orombelli, G., Salloway, J.C., 1985. Quaternary stratigraphy and soil development at the southern border of the Central Alps (Italy): the Bagaggera sequence. Rivista Italiana di Paleontologia e Stratigrafia 90, 565–603.

Cremaschi, M., Federoff, N., Guerreschi, A., Huxtable, J., Colombi, N., Castelletti, L., Maspero, A., 1990. Sedimentary and pedological processes in the upper Pleistocene loess of northern Italy: the Bagaggera sequence. Quaternary International 5, 23–38.

Table B2
Bulk composition of detritus from RL17 core and the Paravino composite section.

Sample	Petrofacies	Q	KF	P	Lvf	Lvm	Lcc	Lcd	Lp	Lch	Lms	Lmv	Lmf	Lmb	Lu	Mu	Bi	AP	&HM	*Tot*	MI
Core Bagaggera RL17																					
4.5	B4	64	2	7	7	2	0	0	1	1	3	1	7	0	0	3	2	0	1	*100.0*	209
7.8	B2b	84	6	1	2	0	1	0	1	3	1	0	0	0	0	1	1	0	0	*100.0*	144
14.3	B3	24	1	0	0	0	29	32	11	1	2	0	1	0	0	0	1	0	0	*100.0*	66
17.2	B3	21	1	1	1	0	35	26	8	2	2	0	1	0	0	0	0	0	0	*100.0*	80
22.6	B3	17	2	2	1	0	31	27	12	2	2	1	2	0	0	0	0	0	0	*100.0*	81
23.5	B3	17	1	2	2	0	45	24	7	1	2	0	0	0	0	0	0	0	0	*100.0*	63
38.7	B3	27	2	2	2	0	33	23	4	2	1	0	3	0	0	1	1	0	0	*100.0*	124
41.0	B2a	79	8	3	5	0	0	0	0	0	1	0	1	0	0	0	2	0	0	*100.0*	117
41.3	B2a	79	11	5	1	0	0	1	0	2	1	0	0	0	0	0	0	0	0	*100.0*	n.d.
45.6	B1	36	9	8	0	0	10	18	0	1	0	0	2	0	0	8	6	0	0	*100.0*	n.d.
Paravino composite section																					
6Cb	P2	63	1	4	7	1	0	0	2	0	3	2	11	0	0	1	3	0	1	*100.0*	203
7Ca	P2	39	0	3	4	3	28	0	3	3	2	0	5	0	0	3	3	2	3	*100.0*	190
6Ca	P1	19	0	1	3	0	47	0	27	2	0	0	1	0	0	0	0	0	0	*100.0*	18
5Cg	P1	15	0	3	2	2	39	0	15	22	0	0	2	0	0	0	0	0	0	*100.0*	44
5Cf	P1	18	1	1	2	0	59	0	13	5	0	0	0	0	0	0	0	0	1	*100.0*	0
5Cd	P1	14	0	0	0	0	61	0	17	3	3	0	2	0	0	0	0	0	1	*100.0*	38
5Cc	P1	17	0	0	3	0	62	0	13	3	0	0	2	0	0	0	0	0	0	*100.0*	21
5Ca	P1	14	0	1	0	0	58	0	15	6	2	0	5	0	0	0	0	0	0	*100.0*	73

Q = quartz; KF = K-feldspar; P = plagioclase; L = lithic grains (Lvf = felsic volcanic; Lvm = intermediate and mafic volcanic; Lcc = limestone; Lcd = dolostone; Lp = shale/siltstone; Lch = chert; Lm = metamorphic; Lu = serpentineschist); Mu = muscovite; Bi = biotite; AP = amphiboles and pyroxenes; &HM = other heavy minerals. MI = Metamorphic Index (Garzanti and Vezzoli, 2003).

Dubar, M., Semah, F., 1986. Paleomagnetic data bearing on the age of high terrace deposits (durance sequence) in Alpine valleys of southeastern France. Quaternary Research 25, 387–391.
Elhers, J., Gibbard, P.L., 2004. Quaternary Glaciations – Extent and Chronology. Part I. Developments in Quaternary Sciences 2, Elsevier, Europe.
Eyles, N., Menzies, J., 1983. The subglacial landsystem. In: Eyles, N. (Ed.), Glacial Geology. Pergamon Press, Oxford, pp. 19–70.
Fink, J., 1979. Paleomagnetic research in the northern foothills of the Alps and in the Vienna basin. Acta Geologica Academiae Scientiarum Hungaricae 22, 111–124.
Galbiati, B., 1969. Stratigrafia e tettonica delle colline di Montevecchia e Lissolo (Brianza orientale). Atti dell'Istituto di Geologia Università di Pavia 20, 101–119.
Garzanti, E., Vezzoli, G., 2003. A classification of metamorphic grains in sandstones based on their composition and grade. Journal of Sedimentary Research 73, 830–837.
Garzanti, E., Andò, S., Vezzoli, G., 2006. The continental crust as a source of sand (Southern Alps cross-section, Northern Italy). Journal of Geology 114, 533–554.
van Geel, B., 1978. A palaeocological study of Holocene peat bog sections in Germany and the Netherlands. Review of Palaeobotany and Palynology 25, 1–120.
van Geel, B., Bohncke, S.J.P., Dee, H., 1981. A palaeocological study of an upper late glacial and holocene sequence from "De Borchert", The Netherlands. Review of Palaeobotany and Palynology 31, 367–448.
Gelati, R., Passeri, L.D., 1967. Il Flysch di Bergamo: nuova formazione cretacica delle Prealpi Lombarde. Rivista Italiana di Paleontologia e Stratigrafia 73, 835–850.
Gibbons, A.B., Megeath, J.D., Pierce, K.L., 1984. Probability of moraine survival in a succession of glacial advances. Geology 12, 327–330.
Head, M.J., Gibbard, P.L., 2005. Early-middle pleistocene transitions: an overview and recommendation for the defining boundary. In: Head, M.J., Gibbard, P.L. (Eds.), Early-Middle Pleistocene Transitions: The Land–Ocean Evidence. Geological Society, London, Special Publication, vol. 247, pp. 1–18.
Häuselmann, P., Fiebig, M., Kubik, P.W., Adrian, H., 2007. A first attempt to date the original "Deckenschotter"' of Penck and Brückner with cosmogenic nuclides. Quaternary International 164-165, 33–42.
Ingersoll, R.V., Bullard, T.F., Ford, R.L., Grimm, J.P., Pickle, J.D., Sares, S.W., 1984. The effect of grain size on detrital modes: a test of the Gazzi-Dickinson point-counting method. Journal of Sedimentary Petrology 54, 103–106.
Jouzel, J., Masson-Delmotte, V., Cattani, O., Dreyfus, G., Falourd, S., Hoffmann, G., Minster, B., Nouet, J., Barnola, J.M., Chappellaz, J., Fischer, H., Gallet, J.C., Johnsen, S., Leuenberger, M., Loulergue, L., Luethi, D., Oerter, H., Parrenin, F., Raisbeck, G., Raynaud, D., Schilt, A., Schwander, J., Selmo, E., Souchez, R., Spahni, R., Stauffer, B., Steffensen, J.P., Stenni, B., Stocker, T.F., Tison, J.L., Werner, M., Wolff, E.W., 2007. Orbital and millennial Antarctic climate variability over the past 800,000 years. Science 317, 793–796.
Kent, D.V., Rio, D., Massari, F., Kukla, G., Lanci, L., 2002. Emergence of Venice during the Pleistocene. Quaternary Science Reviews 21, 1718–1727.
Kirschvink, J.L., 1980. The least squares line and plane and the analysis of paleomagnetic data. Royal Astronomical Society Geophysical Journal 62, 699–718.
Kleboth, P., 1982. Stratigraphie und Sedimentologie der höheren Oberkreide und des Altertiärs der Brianza (Provinz Como, Italien). Memorie di Scienze Geologiche 35, 213–292.
Lisiecki, L.E., Raymo, M.E., 2005. A Pliocene-Pleistocene stack of 57 globally distributed benthic $\delta^{18}O$ records. Paleoceanography 20, PA1003. doi:10.1029/2004PA001071.
Lowrie, W., 1990. Identification of ferromagnetic minerals in a rock by coercivity and unblocking temperature properties. Geophysical Research Letters 17, 159–162.
Mandier, P., 1984. Le relief de la moyenne vallée du Rhône au Tertiaire et au Quaternaire. Université de Lyon II, Lyon.
Massari, F., Rio, D., Serandrei Barbero, R., Asioli, A., Capraro, L., Fornaciari, E., Vergerio, P.P., 2004. The environment of Venice area in the past two million years. Palaeogeography, Palaeoclimatology, Palaeoecology 202, 273–308.
McFadden, P.L., Reid, A.B., 1982. Analysis of palaeomagnetic inclination data. Geophysical Journal of the Royal Astronomical Society 69, 307–319.
Miall, A.D., 2006. The Geology of Fluvial Deposits. 4th corrected printing. Springer, Berlin.
Monegato, G., Ravazzi, C., Donegana, M., Pini, R., Calderoni, G., Wick, L., 2007. Evidence of a two-fold glacial advance during the last glacial maximum in the tagliamento end moraine system (SE Alps). Quaternary Research 68, 284–302.
Moore, P.D., Webb, J.A., Collinson, M.E., 1991. Pollen Analysis. Blackwell Scientific Publications, Oxford.
Moscariello, A., Ravazzi, C., Brauer, A., Mangili, C., Chiesa, S., Rossi, S., De Beaulieu, J.-L., Reille, M., 2000. A long lacustrine record from the Pianico-Sellere basin (middle-late Pleistocene, Northern Italy). Quaternary International 73/74, 47–68.
Muttoni, G., Carcano, C., Garzanti, E., Ghielmi, M., Piccin, A., Pini, R., Rogledi, S., Sciunnach, D., 2003. Onset of major Pleistocene glaciations in the Alps. Geology 31, 989–992.
Muttoni, G., Ravazzi, C., Breda, M., Laj, C., Kissel, C., Mazaud, A., Pini, R., Garzanti, E., 2007. Magnetostratigraphy of the Leffe lacustrine succession (Southern Alps, Italy): evidence for an intensification of glacial activity in the Alps at Marine Isotope Stage 22 (0.87 Ma). Quaternary Research 67, 161–173.
Müllenders, W., Favero, V., Coremans, M., Dirickx, M., 1996. Analyses polliniques de sondages à Venise. Aardkundige Mededelingen 7, 8–117.
Orombelli, G., 1979. Il Ceppo dell'Adda: revisione stratigrafica. Rivista Italiana di Paleontologia e Stratigrafia 85, 573–652.
Orombelli, G., Gnaccolini, M., 1978. Composizione petrografica e provenienza del "ceppo" di Paderno d'Adda. Quaderni del Gruppo di Studio del Quaternario Padano 4, 3–30.
Pavich, M.J., Vidic, N., 1993. Application of paleomagnetic and ^{10}Be analyses to chronostratigraphy of Alpine galcio-fluvial terraces, Sara river valley, Slovenia. Geophysical Monograph 78, 263–275.
Penck, A., Brückner, E., 1909. Die Alpen in Eiszeiten. Tauchnitz, Leipzig.
Pini, R., Ravazzi, C., Orombelli, G., 2003. Le "argille sotto il Ceppo" di Paderno d'Adda: nuovi dati palinologici e biostratigrafici. Rendiconti Istituto Lombardo Scienze Lettere Arti Serie B 136, 93–122.
Pini, R., Ravazzi, C., Donegana, M., 2009. Pollen stratigraphy, vegetation and climate history of the last 215 ka in the Azzano Decimo core (plain of Friuli, north-eastern Italy). Quaternary Science Reviews 28, 1268–1290.
Pugin, A., Bézat, E., Weidmann, M., Wildi, W., 1993. Le bassin d'Ecoteaux (Vaud, Suisse): Témoin de trois cycles glaciaires quaternaires. Eclogae Geologicae Helvetiae 86, 343–354.
Punt, W., Blackmore, S., 1976–2004. The Northwest European Pollen Flora. I-VIII. Elsevier, Amsterdam.
Ravazzi, C., Rossignol Strick, M., 1995. Vegetation change in a climatic cycle of Early Pleistocene age in the Leffe basin (Northern Italy). Palaeogeography, Palaeoclimatology, Palaeoecology 117, 105–122.
Ravazzi, C., Pini, R., Muttoni, G., Breda, M., Chiesa, S., Confortini, F., Egli, R., Martinetto, E., 2005. The lacustrine deposits of Fornaci di Ranica (late Early Pleistocene, Italian Pre-Alps): stratigraphy, palaeoenvironment and geological evolution. Quaternary International 131, 35–58.
Reille, M., 1992–1995. Pollen et spores d'Europe et d'Afrique du Nord. Laboratoire de Botanique historique et Palynologie, Marseille.
Rossi, S., 2003. Analyse pollinique de la séquence lacustre Pleistocène de Planico-Sellere (Italie). PhD thesis, University of Aix-Marseille III/University of Milan.
Riva, A., 1957. Gli anfiteatri morenici a sud del Lario e le pianure diluviali tra Adda e Olona. Atti dell'Istituto Geologico dell'Università di Pavia 7, 5–95.
Sagnotti, L., Winkler, A., 1999. Rock magnetism and palaeomagnetism of greigite-bearing mudstones in the Italian peninsula. Earth and Planetary Science Letters 165, 67–80.
Scardia, G., Muttoni, G., Sciunnach, D., 2006. Subsurface magnetostratigraphy of Pleistocene sediments from the Po Plain (Italy): constraints on rates of sedimentation and rock uplift. Geological Society of America Bulletin 118, 1299–1312.
Shackleton, N.J., et al., 1995. New data on the evolution of Pliocene climate variability. In: Vrba, E. (Ed.), Palaeoclimate and Evolution, with Emphasis on Human Origins. Yale University Press, New Haven, pp. 242–248.
Šibrava, V., 1986. Correlation of European glaciations and their relation to deep sea record. Quaternary Science Reviews 5, 433–442.
Stockmarr, J., 1971. Tablets with spores used in absolute pollen analysis. Pollen and Spores 13, 615–621.
Strini, A., 2001. Gli "occhi pollini" nella Brianza orientale: genesi ed evoluzione nel quadro geologico regionale. PhD thesis, University of Milan.
Tauxe, L., 2005. Inclination flattening and the geocentric axial dipole hypothesis. Earth and Planetary Science Letters 233, 247–261.
Thomas, G.S.P., Connell, R.J., 1985. Iceberg drop, dump and grounding structures from Pleistocene glacio-lacustrine sediments, Scotland. Journal of Sedimentary Research 55, 243–249.
Trautmann, W., 1953. Zur Unterscheidung fossiler Spaltöffnungen der mitteleuropäischen Coniferen. Flora 140, 523–533.
Tzedakis, P.C., 2007. Seven ambiguities in the Mediterranean palaeoenvironmental narrative. Quaternary Science Reviews 26, 2042–2066.
Venzo, S., 1948. Rilevamento geomorfologico dell'apparato morenico dell'Adda di Lecco. Atti della Società Italiana di Scienze Naturali 87, 79–140.
Venzo, S., 1952. Geomorphologische Aufnahme des Pleistozäns (Villafranchian–Würm) im Bergmasker Gebiet und in der östlichen Brianza: Stratigraphie, Palaontologie und Klima. Geologische Rundschau 40, 109–125.
Vezzoli, G., Garzanti, E., 2009. Tracking paleodrainage in Pleistocene foreland basins. Journal of Geology 117, 445–454.
Weltje, G.J., 1997. End-member modelling of compositional data: numerical statistical algorithms for solving the explicit mixing problem. Mathematical Geology 29, 503–549.
Weltje, G.J., 2002. Quantitative analysis of detrital modes: statistically rigorous confidence methods in ternary diagrams and their use in sedimentary petrology. Earth Science Reviews 57, 211–253.
Wentworth, C.K., 1922. A scale of grade and class terms for clastic sediments. Journal of Geology 30, 377–392.
Zijderveld, J.D.A., 1967. A.C. demagnetization of rocks: analysis of results. In: Collinson, D.W., Creer, K.M., Runcorn, S.K. (Eds.), Methods in Palaeomagnetism. Elsevier, Amsterdam, pp. 254–286.
Zuffa, G.G. (Ed.), 1985. Provenance of Arenites. Reidel, Dordrecht NATO ASI Ser. C 148.